

Is interpolation benign for random forests?

Ludovic Arnould¹, Claire Boyer^{1,2}, and Erwan Scornet³

¹LPSM, Sorbonne Université, Paris, France

²MOKAPLAN, INRIA Paris

³CMAP, Ecole Polytechnique, Paris, France

Abstract

Statistical wisdom suggests that very complex models, interpolating training data, will be poor at prediction on unseen examples. Yet, this aphorism has been recently challenged by the identification of benign overfitting regimes, specially studied in the case of parametric models: generalization capabilities may be preserved despite model high complexity. While it is widely known that fully-grown decision trees interpolate and, in turn, have bad predictive performances, the same behavior is yet to be analyzed for random forests. In this paper, we study the trade-off between interpolation and consistency for several types of random forest algorithms. Theoretically, we prove that interpolation regimes and consistency cannot be achieved for non-adaptive random forests. Since adaptivity seems to be the cornerstone to bring together interpolation and consistency, we introduce and study interpolating Adaptive Centered Forests, which are proved to be consistent in a noiseless scenario. Numerical experiments show that Breiman’s random forests are consistent while exactly interpolating, when no bootstrap step is involved. We theoretically control the size of the interpolation area, which converges fast enough to zero, so that exact interpolation and consistency occur in conjunction.

1 Introduction

Random Forests (RF) [8] have proven to be very efficient algorithms, especially on tabular data sets. As any machine learning (ML) algorithm, Random Forests and Decision Trees have been analyzed and used according to the overfitting-underfitting trade-off. Regularization parameters have been introduced in order to control the variance while still reducing the bias. For instance, one can increase the variety of the constructed trees (by playing either with bootstrap samples or feature subsampling), or control the tree structure (by limiting either the number of points falling within each leaf or the maximum depth of all trees).

However, the paradigm stating that high model complexity leads to bad generalization capacity has been recently challenged: in particular, deeper and larger neural networks still empirically exhibit high predictive performances [12]. In such situations, overfitting can be qualified of “benign”:

complex models, possibly leading to interpolation of the training examples, still generalizes well on unseen data [4].

Regarding parametric methods, benign overfitting has been exhibited and well understood in linear regression [3, 22, 15]. Many researchers currently study the *implicit bias* or *implicit regularisation* of stochastic gradient (SGD) strategies used during neural network training: the optimization of an over-parametrized one-hidden-layer neural network via SGD will converge to a minimum of minimal norm with good generalization properties in a regression setting [2], or with maximal margin in a classification setting [10].

Regarding non-parametric methods, practitioners have noticed the good performances of high-depth RFs for a long time (by default, several ML libraries, as the popular Scikit-Learn one, grow trees until pure leaves are reached). More recently, the use of interpolating (or very deep) trees for boosting and bagging methods has been advocated in Wyner et al.. Indeed, [24] believe that the *self-averaging* process at hand in RF (or in boosting methods) also produces an implicit regularization which restrains the interpolating algorithm from overfitting. They even argue that interpolation actually provides robustness against noise: (i) the interpolating estimator would grasp the main signal thanks to its averaging ability; (ii) its high complexity would allow it to locally interpolate a noisy point without damaging the estimated function globally. This argument is to put in parallel with the results proved in [6] where they show that an interpolating kernel method using a singular kernel ($K(x) = \|x\|^{-\alpha} \mathbf{1}_{\|x\| \leq 1}$) reaches minimax convergence rate for β -Hölder regular functions.

Contributions In this paper, we study the trade-off between interpolation and consistency for several types of random forest algorithms. Theoretically, we prove that interpolation regimes and consistency cannot be achieved for non-adaptive centered random forests (Section 3). The major problems for combining interpolation and consistency arises from empty cells in tree partitions. Therefore, we study kernel random forests (KeRF) that are built by averaging over all connected data points (Section 4). By neglecting empty cells, these methods are consistent for larger tree depths, which unfortunately does not meet the strict interpolation requirement. Since adaptivity seems to be the cornerstone to bring together interpolation and consistency, we introduce and study interpolating Adaptive Centered Forests (AdaCRF), which are proved to be consistent in a noiseless scenario (Section 5). Numerical experiments show that Breiman random forests are consistent and interpolate exactly, when the whole data set is used to build each tree (Section 6). If bootstrap is used instead, we numerically show that Breiman random forests are consistent but does not interpolate anymore: however each weak learner in the forest is inconsistent while being an interpolator. Finally, we prove that the volume of the interpolation zone for an infinite Breiman RF (without bootstrap) tends to 0 at a polynomial rate in the number of samples n and an exponential rate in the dimension d (Section 6). This supports the idea that the decay of the interpolation volume is fast enough to retrieve consistency despite interpolation. All proofs are given in Appendix A and all details on experiments in Appendix B.

2 Setting

Framework The general framework is the one of nonparametric regression. We assume to be given a *training set* $\mathcal{D}_n := ((X_1, Y_1), \dots, (X_n, Y_n))$, composed of i.i.d. copies of the generic random variable (X, Y) , where $X \in [0, 1]^d$ is the input and $Y \in \mathbb{R}$ is the output. The underlying model is assumed to satisfy $Y = f^*(X) + \varepsilon$, where $f^*(x) = \mathbb{E}[Y|X = x]$ is the regression function and ε is a random centered noise of variance $\sigma^2 < \infty$. Given an input vector x , the goal is then to predict the associated square integrable random response by estimating $f^*(x)$. We measure the performance of any estimator m_n via its quadratic risk defined as $\mathcal{R}(m_n) := \mathbb{E}[(m_n(x) - f^*(x))^2]$. The asymptotic performance of an estimator m_n is assessed via its *consistency*, a property stating that $\lim_{n \rightarrow \infty} \mathcal{R}(m_n) = 0$.

Estimator A Random Forest (RF) is a predictor consisting of a collection of M randomized trees [see 9, for details about decision trees]. To build a forest, we generate $M \in \mathbb{N}^*$ independent random variables $(\Theta_1, \dots, \Theta_M)$, distributed as a generic random variable Θ , independent of \mathcal{D}_n . In our setting, Θ_j actually represents the successive random splitting directions and the resampling data mechanism in the j -th tree. The predicted value at the query point x given by the j -th tree is defined as

$$m_n(x, \Theta_j) = \sum_{i=1}^n \frac{\mathbb{1}_{X_i \in A_n(x, \Theta_j)} Y_i}{N_n(x, \Theta_j)} \mathbb{1}_{N_n(x, \Theta_j) > 0}$$

where $A_n(x, \Theta_j)$ is the cell containing x and $N_n(x, \Theta_j)$ is the number of points falling into $A_n(x, \Theta_j)$. The (finite) forest estimate then results from the aggregation of M trees:

$$m_{M,n}(x, \Theta_M) = \frac{1}{M} \sum_{j=1}^M m_n(x, \Theta_j),$$

where $\Theta_M := (\Theta_1, \dots, \Theta_M)$. By making the number M of trees grows towards infinity, we can consider instead the *infinite* forest estimate, which has also played an important role in the theoretical understanding of forests:

$$m_{\infty,n}(x) = \mathbb{E}_{\Theta}[m_n(x, \Theta)],$$

where \mathbb{E}_{Θ} denotes the expectation w.r.t. Θ , conditional on \mathcal{D}_n . This operation is justified by the law of large numbers [see 20, for more details].

Several random forests have been proposed depending on the type of randomness they contain (what Θ represents) and the type of decision trees they aggregate. Breiman forest is one of the most widely used random forests, which exhibits excellent predictive performances. Unfortunately, its behavior is difficult to theoretically analyze, because of the numerous complex mechanisms involved in the predictive process (data resampling, data-dependent splits, split randomization). Therefore, in this paper, we simultaneously study the consistency and interpolation properties of different simplified versions of RF, both adaptive (i.e. when trees are built in a data-dependent manner) and non-adaptive.

All forests include a *depth* parameter, denoted k_n , which limits the maximum length of each branch in a tree, hence limiting the number of leaves (up to 2^{k_n}). In this work, we analyze how the tuning of k_n allows us to adjust the *consistency* and *interpolation* characteristics of the forest. The classical notion of (exact) interpolation is defined below.

Definition 2.1 ((Exact) interpolation). An estimator m_n is said to *interpolate* if for all training data (X_i, Y_i) , we have $m_n(X_i) = Y_i$ almost surely.

Recall that the prediction of a single tree at a point x is given by the average of all Y_i such that X_i is contained in the leaf of x . Therefore, each tree within a forest can be parameterized in order to interpolate: it is sufficient to grow the tree until pure leaves (i.e. leaves containing labels of the same values) are reached. In any regression model with continuous random noise, we have $Y_i \neq Y_j$ for all $i \neq j$ almost surely. Therefore, an interpolating tree is a tree that contains at most one point per leaf.

As the final prediction of the random forest is made by averaging the predictions of all its trees, if all trees interpolate, the random forest interpolates as well. Consequently, throughout all the theoretical analysis, we consider RF built without sub-sampling: each tree is built using the whole dataset instead of bootstrap samples as in standard RF. We will discuss the empirical effect of bootstrap in Section 6.

We start our analysis of interpolation and consistency of RF with the simple yet widely studied Centered Random Forest (CRF).

3 Centered RF

Centered Random Forests [7] are ensemble methods that are said to be non-adaptive since trees are built independently of the data: at each step of a centered tree construction, a feature is uniformly chosen among all possible d features and the split along the chosen feature is made at the center of the current cell. Then trees are aggregated to produce a CRF. For CRF, forest interpolation is equivalent to tree interpolation, as shown below.

Lemma 3.1. *The CRF $m_{M,n}$ interpolates if and only if all trees that compose the CRF interpolate.*

Since CRF construction is non-adaptive, it is impossible to enforce exactly one observation per leaf. Hence trees do not interpolate and in turn, the interpolation regime (Definition 2.1) cannot be satisfied for CRF. This leads us to examine a weaker notion of interpolation in probability.

Proposition 3.2 (Probability of interpolation for a centered tree). *Denote \mathcal{I}_T the event “a centered tree of depth k_n interpolates the training data”. Then, for all $n \geq 3$, fixing $k_n = \lfloor \log_2(\alpha_n n) \rfloor$, with $\alpha_n > 1$, one has*

$$e^{-\frac{n}{\alpha_n - 1}} \leq \mathbb{P}(\mathcal{I}_T) \leq e^{-\frac{n}{2(\alpha_n + 1)}}.$$

According to Proposition 3.2, the probability that a tree interpolates tends to one if and only if $k_n = \lfloor \log_2(\alpha_n n) \rfloor$ with $\alpha_n = \omega(n)$ ¹. Consequently, the regime $\alpha_n = \omega(n)$ completely characterizes the interpolation of a centered tree. Proposition 3.2 can be in turn used to control the interpolation probability of a centered RF.

Corollary 3.3 (Probability of interpolation for a CRF). *We denote \mathcal{I}_F the event “a centered forest $m_{M,n}(\cdot, \Theta_M)$ interpolates”. Then, for $k_n = \lfloor \log_2(\alpha_n n) \rfloor$ with $\alpha_n \geq 1$,*

$$\mathbb{P}(\mathcal{I}_F) \leq e^{-\frac{n}{2(\alpha_n+1)}}. \quad (1)$$

According to Corollary 3.3, the condition $\alpha_n = \omega(n)$ (corresponding to the interpolation of a single centered tree with an overwhelming probability) is necessary to ensure that w.h.p., the forest interpolates. Our analysis stresses out that a tree depth of at least $k_n = 2 \log_2(n)$ is required to obtain tree/forest interpolation.

In fact, choosing k_n of the order of $\log_2(n)$ characterizes another type of interpolation regime. To see this, consider a centered tree of depth k , whose leaves are denoted L_1, \dots, L_{2^k} . The number of points falling into the leaf L_i is denoted $N_n(L_i)$. If X is uniformly distributed over $[0, 1]^d$, then by construction, for a given leaf L_i ,

$$\mathbb{P}(X \in L_i) = \frac{1}{2^k} \quad \text{and} \quad \mathbb{E}[N_n(L_i)] = \frac{n}{2^k}. \quad (2)$$

Definition 3.4 (Mean interpolation regime). A CRF $m_{M,n}$ satisfies the *mean interpolation regime* when each tree of $m_{M,n}$ has at least n leaves.

The mean interpolation regime is met for CRF if and only if $k_n \geq \log_2 n$. By Equation (2), this implies that for all leaves L_i , $\mathbb{E}[N_n(L_i)] \leq 1$, that is each leaf contains at most one point in expectation. Therefore, one could say that trees interpolate in expectation in the mean interpolation regime.

In both interpolation regimes (mean and in probability), trees need to be very deep, with a growing number of empty cells as n tends to infinity, eventually damaging the consistency of the overall CRF.

Proposition 3.5. *Suppose that $\mathbb{E}[f(X)^2] > 0$. Then the infinite Centered Random Forest of depth $k_n \geq \lfloor \log_2 n \rfloor$ is inconsistent.*

The non-consistency of the CRF stems from the fact that the probability for a random point X to fall in an empty cell does not converge to zero, introducing an irreducible bias in the excess risk.

Proposition 3.5 emphasizes the poor generalisation capacities of the interpolating CRF (under any interpolating regime), which could be expected given its non-adaptive construction. Since controlling empty cells seems crucial for the consistency, this motivates the analysis of kernel RFs (KeRF), in which empty cells are not taken into account for the prediction at x (unless all cells containing x are empty across all trees in the forest).

¹i.e. α_n asymptotically dominates n .

4 Centered kernel RF

As formalized in [11] and developed in [1], slightly modifying the aggregation rule of tree estimates provides a kernel-type estimator. Instead of averaging the predictions of all centered trees, the construction of a kernel RF (KeRF) is performed by growing all centered trees and then averaging along all points contained in the leaves in which x falls, i.e.

$$\tilde{m}_{M,n}(x, \Theta_M) := \frac{\sum_{i=1}^n Y_i \sum_{j=1}^M \mathbb{1}_{X_i \in A_n(x, \Theta_j)}}{\sum_{i=1}^n \sum_{j=1}^M \mathbb{1}_{X_i \in A_n(x, \Theta_j)}}.$$

One of the benefits of this construction is to limit the influence of empty cells, which can be harmful for both consistency and interpolation (see Section 3). Letting $K_{M,n}$ be the connection function of the M finite forest defined by

$$K_{M,n}(x, \mathbf{z}) := \frac{1}{M} \sum_{j=1}^M \mathbb{1}_{\mathbf{z} \in A_n(x, \Theta_j)},$$

[21] shows that the KeRF can be rewritten as

$$\tilde{m}_{M,n}(x, \Theta_M) = \frac{\sum_{i=1}^n Y_i K_{M,n}(x, \mathbf{X}_i)}{\sum_{i=1}^n K_{M,n}(x, \mathbf{X}_i)},$$

hence the name of kernel RF. In addition, it is shown that

$$\lim_{M \rightarrow \infty} K_{M,n}(x, z) := K_n(x, z),$$

where $K_n(x, z) = \mathbb{P}_{\Theta} [z \in A_n(x, \Theta)]$ which can be seen as the empirical probability for x and z to be in the same cell w.r.t. a tree built according to Θ . Consequently, for all $x \in [0, 1]^d$, the infinite KeRF reads as

$$\tilde{m}_{\infty,n}(x) = \frac{\sum_{i=1}^n Y_i K_n(x, X_i)}{\sum_{i=1}^n K_n(x, X_i)}.$$

4.1 Interpolation Conditions

Since KeRF aggregate centered trees as CRF (but in a different way), results from Section 3 can be extended to KeRF:

1. the mean interpolation regime is met for centered trees, and therefore for KeRF, as soon as $k_n \geq \log_2 n$;
2. a necessary condition to attain the KeRF interpolation in probability is $k_n > 2 \log_2(n)$.

One can note that the depths required for both interpolation regimes are still large, leading to as many empty cells for KeRF as for classical CRF but the aggregation rule is such that they are not taken into account in KeRF predictions, which gives hope that consistency could be preserved.

4.2 Consistency

In this section, we study the convergence of the centered KeRF when k_n is of the order of $\log_2(n)$, i.e. under the *mean interpolation regime*. To this end, we consider extra hypotheses on the noise and on the regularity of f^* .

Theorem 4.1. *Assume that f^* is Lipschitz continuous and that the additive noise ε is a centered Gaussian variable with a finite variance σ^2 . Then, the risk of the infinite centered KeRF of depth $k_n = \lfloor \log_2(n) \rfloor$ verifies, for all $n \geq 2$,*

$$\mathcal{R}(\tilde{m}_{\infty,n}) \leq C_d \log(n)^{-(d-11)/6},$$

with $C_d > 0$ a constant depending on $\sigma, d, \|f^*\|_\infty$.

Theorem 4.1 states that the infinite centered KeRF estimator is consistent as soon as $d > 11$, with a slow convergence rate of $\log(n)^{-(d-11)/6}$. The proof is based on the general paradigm of bias-variance trade-off and is adapted from [21]. At first sight, one might think that the rate becomes better as the dimension d increases. This would be without thinking that the constant in front of it depends on the dimension, so that the established bound should be regarded for any fixed d .

Choosing $k_n = \lfloor \log_2(n) \rfloor$ in Theorem 4.1 allows us to have a mean interpolation regime concomitant with consistency for KeRF, therefore highlighting that consistency and mean interpolation are compatible. This is not the case for CRF for which the mean interpolation regime forbids convergence (Proposition 3.5). If a “mean” overfitting regime is benign for the consistency of KeRF, it seems to be nonetheless malignant for the convergence rate. Indeed, Lin and Jeon [16] provides a lower bound on the optimal convergence rate of a non-adaptive RF (such as the CRF), scaling in $(\log n)^{-(d-1)}$. This leads us to believe that the convergence rate we obtain in Theorem 4.1 is marginally improvable.

Interpolation for kernel estimators has been studied recently for singular kernel by [6]. Since KeRF are kernel estimators, one can wonder how sharp is our bound (Theorem 4.1) compared to that of [6], which is minimax. Due to the spikiness of the singular kernel studied in [6], interpolation arises for any kernel bandwidth. The latter can be then tuned to reach minimax rates of consistency. The story is totally different for KeRF since interpolation occurs only for specific tree depths $k_n \geq \log(n)$ (where the depth parameter is closely related to the bandwidth of classical kernel estimates). Less latitude for choosing the depth then leads to sub-optimal rates of consistency (see Theorem 4.1). Of course, a better rate of consistency in $O(n^{1/(3+d \log 2)})$ could be obtained as in [21] when optimizing this depth parameter, but leaving the interpolation world.

4.3 Empirical results

We numerically assess the performance of KeRF in the mean interpolation regime.

Experimental framework We consider four different regression models, most of which have been already considered in [23]: Model 1 is additive without noise ($d = 2$), Model 2 is polynomial

with interactions ($d = 8$), Model 3 is the sum of elementary terms that contain non-polynomial interactions ($d = 6$) and Model 4 ($d = 5$) corresponds to a generalized linear model. All models are specified in Appendix B. For each model, the simulated dataset is divided into a training set (80% of the data set) and a test set (the remaining 20%). We train a centered KeRF (with $M = 500$) of depth fixed to $\lceil \log_2 n \rceil + 1$ (mean interpolation regime) for different sample sizes n and evaluate the empirical quadratic risk on the test set.

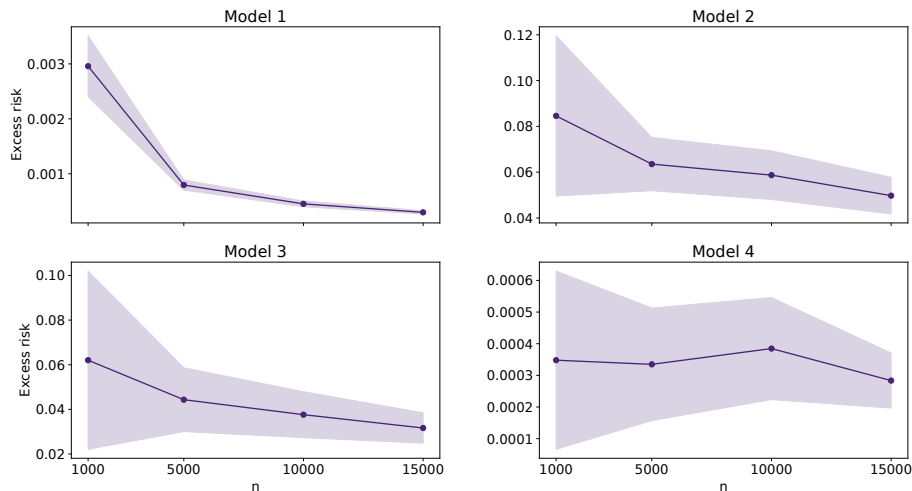


Figure 1: KeRF consistency results: excess risk w.r.t. sample sizes. For each sample size n , the experiment is repeated 30 times: we represent the mean over the 30 tries (bold line) and the mean \pm std (filled zone).

Results On Figure 1, for all models, the risk decreases toward zero as the number of samples n increases (with slow convergence rates). These numerical results, even though obtained for a finite KeRF with a large number $M = 500$ of centered trees, support the theoretical consistency of the infinite KeRF in the mean interpolation regime (see Theorem 4.1).

5 Adaptive CRF

Since consistency can be only analyzed for KeRF in the mean interpolation regime, we introduce a new adaptive tree which reaches the strict interpolation regime. This so-called *adaptive centered tree* is a modified version of a centered tree, built by taking into account the positions of the X_i 's, and thereby reduces the number of empty leaves. It is recursively grown: at each node, a feature is uniformly chosen among the set of all *separable* d features (a feature is separable if cutting this feature produces two non-empty cells) and the split is made in the middle of the current node along the chosen feature. If there are more than one point in the current node and none of the feature separates them, the splitting direction is uniformly chosen among all the separable features of the

previous cut. The construction stops when all leaves contain 0 or 1 observation. The *Adaptive Centered RF* (AdaCRF) results from a specific aggregation of such trees: for a given point x , the final prediction of the RF is given by averaging along all the trees for which x falls into a non-empty leaf.

5.1 Interpolation

By construction, AdaCRF interpolates since all trees interpolate. AdaCRF adaptivity allows it to reach full growth while preserving a reasonable depth in probability. To this aim, we grow an adaptive centered tree and measure, for a given point x , the depth $k_n(x)$ associated to the cell containing x .

Lemma 5.1 (Depth of an adaptive centered tree). *For all $\alpha \in [0, 1)$,*

$$\mathbb{P}(k_n(X) \in [\log(n) \pm \log^{1-\alpha}(n)]) \xrightarrow{n \rightarrow \infty} 1.$$

Lemma 5.1 states that the asymptotic behavior of $k_n(X)$ is equivalent to $\log n$ up to a negligible factor. The $\log(n)$ equivalent matches the condition for the mean interpolation regime in the case of CRF exhibited in Section 3. Therefore, while AdaCRF has a depth of the same order as that of a classical CRF, its adaptivity nature ensures its interpolation. Finally, given AdaCRF flexibility, we go beyond the depth $O((1 - 2 \log_2(1 - \frac{1}{2d}))^{-1} \log_2 n)$, proved to be optimal for classical CRF [14], to establish that AdaCRF is consistent in the $\log n$ regime.

5.2 Consistency

We study the consistency of an interpolating infinite AdaCRF for which we are able to conclude favourably in a noiseless scenario.

Theorem 5.2. *Assume a noiseless setting ($\varepsilon = 0$ a.s.) and suppose that f^* is bounded and has bounded partial derivatives $\partial_j f^*$ for all j . Let M tend to infinity such that $M = o(n^{-\log_2(1-3/4d)})$. Then, the interpolating Adaptive Centered Random Forest with M trees is consistent.*

The proof is adapted from [14]. Theorem 5.2 is the first result to establish the consistency of an interpolating (adaptive) forest, therefore highlighting that consistency and (exact) interpolation are not contradictory for random forests. Note that the consistency achieved by AdaCRF cannot be obtained for non-adaptive CRF under the interpolation regime, even in the noiseless setting, as proved in Section 3. Indeed, the inconsistency of non-adaptive centered random forests results from the non-negligible probability of falling into empty cells, which cannot be coerced under any interpolation regimes.

As a matter of fact, bounding above the probability of falling into an empty cell is a cornerstone to establish Theorem 5.2, even beyond the noiseless setting. This probability decreases in $O(1/n)$ as detailed in the following lemma.

Lemma 5.3. Consider a finite forest $m_{M,n}$ with M trees. Let X be a uniform random variable on $[0, 1]^d, d \geq 2$. We denote \mathcal{E}_M the event “ X falls in an empty leaf for all trees in the forest $m_{M,n}$ ”. Then, for all $n \geq 6$,

$$\mathbb{P}(\mathcal{E}_M) \leq \frac{4M}{2n-1} + \left(1 - \frac{1}{d}\right)^M$$

Letting M tend to infinity as $M = o(n)$ is sufficient to ensure that empty cells are negligible. The stringer condition in Theorem 5.2 results from the additional control of the approximation error of the forest. Analyses of CRF conducted by [7, 14] showed that the probability of falling into an empty cell is upper bounded by $\exp(-n/2^{k_n})$. This leads them to consider the regime $k_n = o(\log_2(n))$, in order to prove the forest consistency. It turns out that the sharp analysis provided by [14] highlights that the probability of falling into empty cells is the only limiting term to reach consistency in the $k_n = \log_2(n)$ regime. This stresses out the importance of Lemma 5.3, to derive the consistency of CRF in a noisy setting.

Following this comment, we firmly believe that Theorem 5.2 also stands in the more general setting of noisy data and that the limitation is mainly due to a technical obstruction within the proof. This intuition is substantiated by a theoretical control of the volume of *interpolation zones* (Section 5.3) and by numerical experiments (Section 5.4).

5.3 Volume of the interpolation area

To go one step further in the analysis of AdaCRF, we introduce the notion of *interpolation area* defined below.

Definition 5.4. The *interpolation area* is the subspace of $[0, 1]^d$ where the prediction of the forest depends on one training point only. For a given forest $m_{M,n}(\cdot, \Theta_M)$, the interpolation area is denoted by

$$\begin{aligned} \mathcal{A}(m_{M,n}(\cdot, \Theta_M)) \\ = \left\{ x \in [0, 1]^d, \exists! X_i \in \mathcal{D}_n, X_i \in \bigcap_{m=1}^M A_n(x, \Theta_m) \right\}. \end{aligned}$$

The interpolation zone heavily depends on both the geometry of the training points X_i 's and the construction of the trees. Analyzing the interpolation area for a finite AdaCRF turns out to be quite a challenging task. Therefore, we focus our study on the *core interpolation area* \mathcal{A}_{min} written as

$$\mathcal{A}_{min} = \bigcap_{M \in \mathbb{N}, \Theta_M} \mathcal{A}(m_{M,n}(\cdot, \Theta_M)).$$

The area \mathcal{A}_{min} is nothing but the intersection of the interpolation zones of all possible forests, or equivalently of a forest containing all the possible trees (and therefore all possible cuts). As an

example note that in the case of centered trees, every cut may occur with a positive probability. Therefore, \mathcal{A}_{min} matches the volume of the interpolation area of an infinite centered AdaCRF. In the following proposition, we control the volume $\mu(\mathcal{A}_{min})$ of the minimal interpolation zone of AdaCRF, where μ is the Lebesgue measure.

Proposition 5.5. *For all $n \geq 2$, for all $d \geq 2$, consider an infinite AdaCRF $m_{\infty,n}$. Then,*

$$\mathbb{E}_{\mathcal{D}_n} [\mu(\mathcal{A}_{min})] \leq \left(\frac{2}{\log 2} \right)^d \frac{(1 - 2^{-n})^d}{n^{d-1}}.$$

The volume of the interpolation area for an infinite AdaCRF tends to 0 polynomially in n and exponentially in d , and so does $\mathbb{E}_{\mathcal{D}_n} [\mathbb{P}(X \in \mathcal{A}_{min})]$. Hence, apart from a very restricted zone, the prediction of the AdaCRF mostly relies on more than one training point. This highlights the predominant *self-averaging* property of such forest architectures, and hence underpins the idea of good capabilities of AdaCRF in interpolation regimes (with or without noise).

5.4 Empirical consistency results

We analyze the empirical performances of AdaCRF in noiseless and noisy settings on the same models as considered in Section 4.3. For each model, given a training set, we train AdaCRF (with $M = 500$ trees) until pure leaves are reached, and measure its excess risk on a test set.

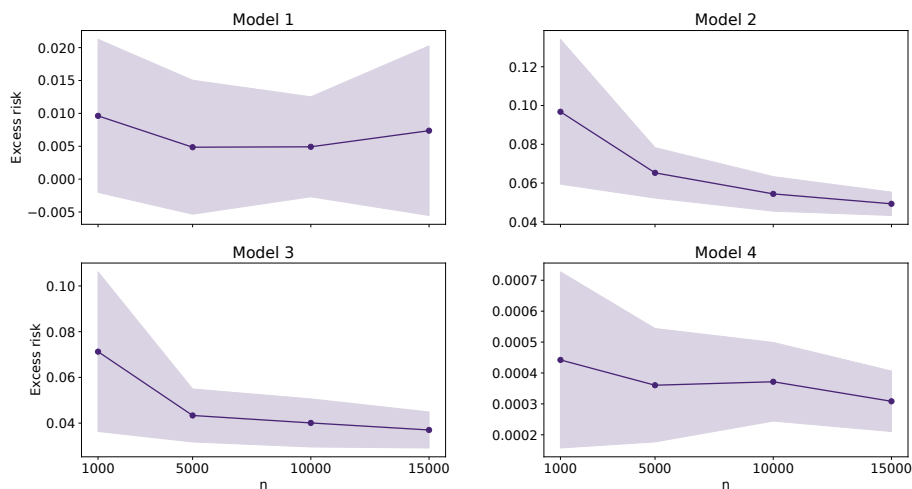


Figure 2: Consistency results for an AdaCRF with $M = 500$ trees: excess risk w.r.t. the sample size n . For each sample size, the experiment is repeated 30 times: we represent the mean over the 30 tries (bold line) and the mean \pm std (filled zone).

Figure 2 shows that the excess risk of AdaCRF decreases as n grows. The particular shape of Model 1 probably results from the absence of noise (the excess risk is still close to zero but with large

variations). These empirical performances lend support to the idea that AdaCRF are consistent even with a finite number of trees and beyond the noiseless setting.

6 Breiman RF

The widely-used Breiman RF is composed of several trees, built with CART methodology, each one trained on bootstrap samples, and for which the successive splitting directions and thresholds are chosen at each step (among a random subset of directions) in order to minimize the CART criterion (empirical variance for instance). Breiman forests are among the state-of-the-art ensemble methods in terms of predictive performance even if their adaptivity to the data remains a real hurdle to their theoretical analysis.

From the interpolation perspective, each CART being trained on a bootstrap sample, the RF interpolation is not ensured when considering fully-grown trees. Indeed, a tree cannot interpolate a point that is not chosen in the bootstrap step. For this reason, we focus our study on the volume of interpolation areas for Breiman RF without bootstrap and then analyze their empirical behavior in interpolating regimes through a battery of numerical experiments.

6.1 Interpolation Conditions

As a Breiman RF is built using both the X_i 's and the Y_i 's, it is hard to determine the depth necessary to reach the interpolation state. Depending on the data, the latter can be of the order $k \approx \log_2(n)$ in the best case, if each cut creates approximately two groups of the same size), or $k \approx n$ in the worst case, if only one point is separated from the others at each step [low signal-to-noise ratios situations, see e.g., 13]. Note that by omitting the bootstrap step in the RF construction, the interpolation of Breiman forests directly results from aggregating fully-grown trees.

6.2 Volume of the interpolation zone

As shown in the next proposition, the volume of the minimal interpolation zone tends to 0 as n tends to infinity.

Proposition 6.1. *Consider an infinite Breiman forest constructed without bootstrap. Suppose that for a given configuration of the training data, all cuts have a probability strictly greater than 0 to appear. Then, the volume of the minimal interpolation zone verifies*

$$\mathbb{E}[\mu(\mathcal{A}_{min})] \leq \frac{1}{n^{d-1}} (1 - 2^{-n})^d.$$

Similarly to the AdaCRF, the bound on the interpolation volume for a Breiman forest enjoys the same order of decay, improved by a constant exponential in the dimension. Since, predictions cannot

be accurate in the interpolation area in a noisy setting, it is necessary that the volume of this area decreases to zero in order to ensure the RF consistency. Proposition 6.1 therefore suggests the good generalization properties of Breiman RF in interpolation regimes, as several training points are mostly used for prediction.

Setting the number of eligible features for splitting to 1 is sufficient to ensure the hypothesis on cuts in Proposition 6.1: one can obtain a tree in which all splits are performed along a single direction. This is a minor modification to the original algorithm and an easy one to implement since most ML libraries have a “max-feature” (as scikit-learn in Python) or “mtry” (in R) parameter that can be set to 1.

6.3 Empirical study

Interpolation volume We numerically evaluate the volume of the interpolation area of a Breiman RF (with 5000 trees, see Figure 10 in Appendix B.2 for details about this choice) when the sample size n increases.

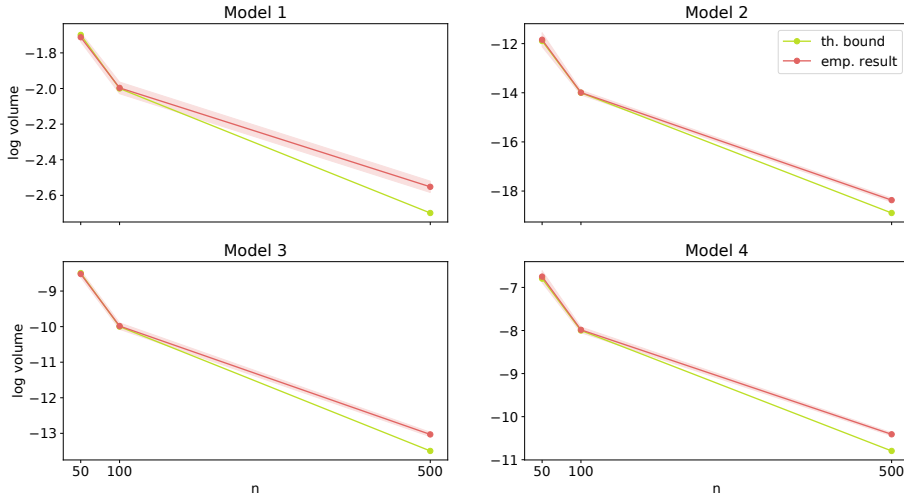


Figure 3: Log volume of the interpolation zone of a Breiman RF with 5000 Trees, max features set to 1, no bootstrap. Mean over 10 tries (red line) and mean \pm std (filled zone). The theoretical bound (Proposition 6.1) is represented in green.

In Figure 3, the volume of the minimal interpolation zone is shown to tend polynomially fast to 0 (linear in the logarithmic scale) for all considered models as the dataset size increases, matching the behavior of the theoretical bound established in Proposition 6.1.

One could notice the slight gap between the theoretical and experimental curves, which actually reflects the gap between an infinite forest (for which Proposition 6.1 holds) and its approximation by a finite forest (5000 trees here). This gap naturally tends to increase with n (when the number

of trees is fixed) as the approximation of the infinite RF by a finite one deteriorates with n .

Consistency We now present an empirical study of Breiman RF consistency in interpolation regimes. In the theoretical analysis, we have focused on a specific type of Breiman RF (with no bootstrap and a *max-features* parameter equal to 1). We now examine the characteristics of Breiman forests with their default parameter and study the regularization processes that limit the noise sensitivity in the interpolation regime.

In order to reach a better estimation of the regression function, Breiman RF averages several CARTs while introducing randomness in the construction of each tree to diversify them. The first randomization comes from the *bootstrap*: each tree is trained on a bootstrap sample (selecting n observations out of the n original ones, with replacement). The other randomization results from a random selection of splitting directions: at each node, a subset of $\{1, \dots, d\}$ of size *max-features* is randomly selected and CART criterion is optimized along these directions only (setting *max-features* to 1 provides the maximum diversity whereas setting it to d results in the construction of a unique tree).

The benefit of these two aspects in the construction of the Breiman RF is numerically analyzed when using interpolating Breiman trees. In Figure 4, we measure the excess risk of two RFs with 500 trees and *max-depth= None*, where for the first one, bootstrap is used and the *max-features* parameter is set to 1, whereas the second one excludes bootstrap and set the *max-features* parameter to $\lceil d/3 \rceil$ (default value in `randomForest` in R).

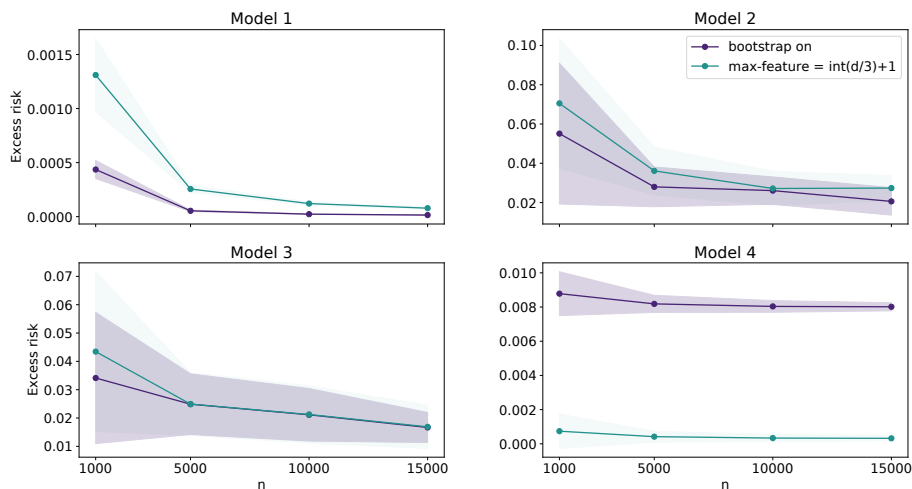


Figure 4: Consistency of two Breiman RF: excess risk w.r.t. sample size n . Parameters : 500 trees per forest, *max-depth= None*, *max-features= d* for the “bootstrap on” RF, bootstrap off for the “max-feature= $\lceil d/3 \rceil$ ” RF. Mean over 30 tries (bold lines) and mean \pm std (filled zone).

In Figure 4, we observe that the excess risk decreases to 0 for all models and for both forests. Indeed, each randomizing process alone induces enough diversity across trees for the self-averaging property

to be efficient, resulting in the consistency of the overall forests [see also 20, 17, 18, for insights about tree diversity in random forests].

However, when using bootstrap, consistency comes at the cost of leaving the interpolation regime, as only $2/3$ of the data are used in average to build each tree (see Figures 11, 12 in Section B.2.3 for more details about the forest non-interpolation). In regards of this internal sampling selection, the aggregation of interpolating bagged trees results in smoothing the decision process of the entire forest, providing thereby a consistent but not interpolating estimate.

In turn, Breiman RF built with $max\text{-features} = \lceil d/3 \rceil$ seems consistent while preserving its interpolating behavior. Within this configuration, the final RF still interpolates the data but the volume of the interpolation zone is very small as shown in Figure 9. This is in line with the vision of a *locally spiky* estimator developed in [24] and [4]. Indeed, the influence of the averaging effect is locally null near the data training points, but increases with the distance from these points. Note that bootstrap and feature subsampling act differently. Bootstrap smoothens predictions by averaging different observations, even at points of the training set, which leads to an empty interpolation area. On the other hand, feature subsampling increases tree partition diversity, which reduces but does not annihilate the interpolation area of the overall forest.

In this regard, Breiman RF with $max\text{-features} = \lceil d/3 \rceil$ are similar to interpolating *spiky* non-singular kernel methods, as the ones introduced in [6], except for the leeway allowed for the hyperparameters tuning. Indeed, as underlined for non-adaptive centered forests, the depth k_n (i.e. the tuned parameter) is constrained to a strict range to ensure both consistency and interpolation. This is not the case for singular kernel methods, as they interpolate regardless of the window parameter value.

7 Conclusion

In this paper, we study both empirically and theoretically the tradeoff between interpolation and consistency of different types of random forests. In particular, we show that interpolation is harmless in the case of adaptive methods when the *self-averaging* process in the forest is sufficient to restrain the interpolation effect to a local influence.

Indeed, we prove that the AdaCRF reaches consistency and exact interpolation regimes in a noiseless scenario. This is the first result to prove that consistency and interpolation are not irreconcilable for such powerful learners. Breiman forests is also shown empirically to be consistent and interpolate when no bootstrap step is involved. This results from a fast decrease of the interpolation area, which limits the negative impact of interpolation on the overall consistency of the method.

We believe that the analysis of the interpolation zone of RF introduced in this article is a milestone for the understanding of RF prediction in interpolation regimes. Indeed the volume of the interpolation area is actually a roundabout way to measure the diversity in the constructed trees: if this volume is high, all trees end up building similar partitions.

Studying the impact of max-feature on the interpolation area volume is also a promising way to

gain a better understanding of the role of this parameter in random forests.

References

- [1] Sylvain Arlot and Robin Genuer. Analysis of purely random forests bias. *arXiv preprint arXiv:1407.3939*, 2014.
- [2] Francis Bach and Lenaïc Chizat. Gradient descent on infinitely wide neural networks: Global convergence and generalization, 2021.
- [3] Peter L Bartlett, Philip M Long, Gábor Lugosi, and Alexander Tsigler. Benign overfitting in linear regression. *Proceedings of the National Academy of Sciences*, 117(48):30063–30070, 2020.
- [4] Peter L Bartlett, Andrea Montanari, and Alexander Rakhlin. Deep learning: a statistical viewpoint. *arXiv preprint arXiv:2103.09177*, 2021.
- [5] Necdet Batir. Inequalities for the gamma function. *Archiv der Mathematik*, 91(6):554–563, 2008.
- [6] Mikhail Belkin, Alexander Rakhlin, and Alexandre B Tsybakov. Does data interpolation contradict statistical optimality? In *The 22nd International Conference on Artificial Intelligence and Statistics*, pages 1611–1619. PMLR, 2019.
- [7] Gérard Biau. Analysis of a random forests model. *The Journal of Machine Learning Research*, 13:1063–1095, 2012.
- [8] Leo Breiman. Random forests. *Machine learning*, 45(1):5–32, 2001.
- [9] Leo Breiman, Jerome Friedman, Charles J Stone, and Richard A Olshen. *Classification and regression trees*. CRC press, 1984.
- [10] Lenaïc Chizat and Francis Bach. Implicit bias of gradient descent for wide two-layer neural networks trained with the logistic loss. In *Conference on Learning Theory*, pages 1305–1338. PMLR, 2020.
- [11] Pierre Geurts, Damien Ernst, and Louis Wehenkel. Extremely randomized trees. *Machine learning*, 63(1):3–42, 2006.
- [12] Ian Goodfellow, Yoshua Bengio, and Aaron Courville. *Deep learning*. MIT press, 2016.
- [13] Hemant Ishwaran. The effect of splitting on random forests. *Machine learning*, 99(1):75–118, 2015.
- [14] Jason Klusowski. Sharp analysis of a simple model for random forests. In *International Conference on Artificial Intelligence and Statistics*, pages 757–765. PMLR, 2021.
- [15] Tengyuan Liang, Alexander Rakhlin, and Xiyu Zhai. On the multiple descent of minimum-norm interpolants and restricted lower isometry of kernels. In *Conference on Learning Theory*, pages 2683–2711. PMLR, 2020.

- [16] Yi Lin and Yongho Jeon. Random forests and adaptive nearest neighbors. *Journal of the American Statistical Association*, 101(474):578–590, 2006.
- [17] Lucas Mentch and Siyu Zhou. Randomization as regularization: a degrees of freedom explanation for random forest success. *arXiv preprint arXiv:1911.00190*, 2019.
- [18] Jaouad Mourtada, Stéphane Gaïffas, and Erwan Scornet. Minimax optimal rates for mondrian trees and forests. *The Annals of Statistics*, 48(4):2253–2276, 2020.
- [19] Lawrence Bruce Richmond and Jeffrey Shallit. Counting abelian squares. *arXiv preprint arXiv:0807.5028*, 2008.
- [20] Erwan Scornet. On the asymptotics of random forests. *Journal of Multivariate Analysis*, 146:72–83, 2016.
- [21] Erwan Scornet. Random forests and kernel methods. *IEEE Transactions on Information Theory*, 62(3):1485–1500, 2016.
- [22] Alexander Tsigler and Peter L Bartlett. Benign overfitting in ridge regression. *arXiv preprint arXiv:2009.14286*, 2020.
- [23] Mark J Van der Laan, Eric C Polley, and Alan E Hubbard. Super learner. *Statistical applications in genetics and molecular biology*, 6(1), 2007.
- [24] Abraham J Wyner, Matthew Olson, Justin Bleich, and David Mease. Explaining the success of adaboost and random forests as interpolating classifiers. *The Journal of Machine Learning Research*, 18(1):1558–1590, 2017.

A Proofs

A.1 Proofs of Section 3

A.1.1 Proof of Proposition 3.2

As all the leaves have the same volume and the data points are independent and uniformly distributed, having at most one point per leaf is equivalent to distribute n balls into 2^k boxes containing at most one point with $2^k \geq n$ as can be seen on Figure 5.

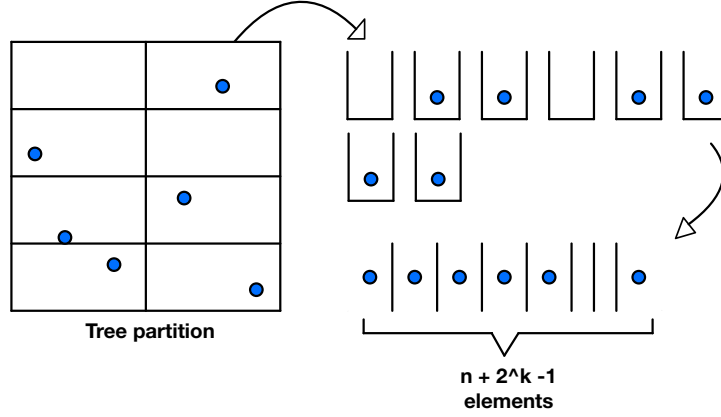


Figure 5: Computing the interpolation probability (depth $k = 3$, $n = 6$)

Thus

$$\begin{aligned} \mathbb{P}(\mathcal{I}_T) &= \frac{\binom{2^k}{n}}{\binom{n+2^k-1}{n}} \\ &= \frac{2^k!}{(2^k - n)!n!} \frac{n!(2^k - 1)!}{(n + 2^k - 1)!}. \end{aligned}$$

With $k = \lfloor \log_2(\alpha_n n) \rfloor \in \mathbb{N}$, we have

$$\mathbb{P}(\mathcal{I}_T) = \frac{\alpha_n n}{(\alpha_n + 1)n - 1} \cdot \frac{\alpha_n n - 1}{(\alpha_n + 1)n - 2} \cdots \frac{(\alpha_n - 1)n + 1}{\alpha_n n}.$$

- We begin by computing the lower bound:

$$\begin{aligned} \mathbb{P}(\mathcal{I}_T) &\geq \frac{\alpha_n n}{(\alpha_n + 1)n} \cdot \frac{\alpha_n n - 1}{(\alpha_n + 1)n - 1} \cdots \frac{(\alpha_n - 1)n + 1}{\alpha_n n + 1} \\ &\geq \left(\frac{\alpha_n - 1}{\alpha_n} \right)^n \\ &\geq e^{n \log(1 - \frac{1}{\alpha_n})} \\ &\geq e^{-\frac{n}{\alpha_n - 1}} \xrightarrow{\alpha_n \rightarrow \infty} 1 \end{aligned}$$

- The computation of the upper bound is similar, note that for all $r \in \{0, \dots, n\}$,

$$\frac{\alpha_n n - r}{(\alpha_n + 1)n - r - 1} \leq \frac{\alpha_n + 1/2}{\alpha_n + 1}.$$

It follows that

$$\begin{aligned}\mathbb{P}(\mathcal{I}_T) &\leq \left(\frac{\alpha_n + 1/2}{\alpha_n + 1}\right)^n \\ &\leq e^{n \log(\frac{\alpha_n + 1/2}{\alpha_n + 1})} \\ &\leq e^{-\frac{n}{2(\alpha_n + 1)}}.\end{aligned}$$

A.1.2 Proof of Lemma 3.1

Suppose that a tree m_r in the forest does not interpolate for a given point $X_s, s \in \{1, \dots, n\}$, we write $m_r(X_s, \Theta_r) = Y_s + \xi$, $\xi \neq 0$. Then, by definition of $m_{M,n}$,

$$\begin{aligned}m_{M,n}(X_s, \Theta_M) &= \frac{1}{M} \sum_{j=1}^M \sum_{i=1}^n Y_i W_{ij} \\ &= \frac{1}{M} \sum_{j=1, j \neq r}^M \sum_{i=1}^n (f^*(X_i) + \varepsilon_i) W_{ij} + \frac{1}{M} (Y_s + \xi)\end{aligned}$$

where $W_{ij} := \frac{\mathbb{1}_{X_i \in \mathcal{A}_n(X_s, \Theta_j)}}{N_n(X_s, \Theta_j)} \mathbb{1}_{N_n(X_s, \Theta_j) > 0}$. Therefore, $m_{M,n}(X_s, \Theta_M) = Y_s$ if and only if

$$\begin{aligned}\frac{1}{M} \sum_{j=1, j \neq r}^M \sum_{i=1}^n (f^*(X_i) + \varepsilon_i) W_{ij} + \frac{1}{M} (Y_s + \xi) &= Y_s \\ \iff \frac{1}{M} \sum_{j=1, j \neq r}^M \sum_{i=1}^n (f^*(X_i) + \varepsilon_i) W_{ij} &= -\frac{\xi}{M} \\ \iff \frac{1}{M} \sum_{j=1, j \neq r}^M \sum_{i=1}^n \varepsilon_i W_{ij} &= -\frac{\xi}{M} + C\end{aligned}$$

where C is random and independent from ε_i for all i . ξ was computed with the label noise of at least one point different from X_s (otherwise it would equal 0). We can write

$$\xi = C' + \frac{1}{M} \sum_{i=1}^n \varepsilon_i W_{ir}$$

where C' is independent from the ε_i s. Finally, the forest interpolates at X_s if and only if

$$\frac{1}{M} \sum_{j=1}^M \sum_{i=1}^n \varepsilon_i W_{ij} = C + C'$$

However, as the noise is continuous and independent from W_{ij} for all i, j and from C, C' , this equality happens with a zero probability.

A.1.3 Proof of Corollary 3.3

As it is necessary for all trees to interpolate for the forest to interpolate, the probability that the forest interpolates is smaller than the probability that a single tree interpolates.

A.1.4 Proof of Proposition 3.5

Let $m_{n,\infty}(\cdot)$ be an infinite CRF with each tree containing at least $\alpha_n n$ leaves, with $\alpha_n > 1$. Let X be uniformly distributed on $[0, 1]^d$. We write $\bar{m}_{n,\infty}(X) = \mathbb{E}[m_{n,\infty}(X) | X, X_1, \dots, X_n]$. Then, denoting \mathcal{E} the event

“ $N_{n,\infty}(X) = 0$ ” (or equivalently, “ X falls into a non-empty leaf”),

$$\mathcal{R}(m_{n,\infty}(X)) = \mathbb{E} \left[(m_{n,\infty}(X) - f^*(X))^2 \right] \quad (3)$$

$$\geq \mathbb{E} \left[(\bar{m}_{n,\infty}(X) - f^*(X))^2 \right] \quad (4)$$

$$= \mathbb{E} \left[\left(\sum_{i=1}^n \mathbb{E}_{\Theta} [W_i f(X_i)] - (\mathbb{1}_{\mathcal{E}} + \mathbb{1}_{\mathcal{E}^c}) f^*(X) \right)^2 \right] \quad (5)$$

$$= \mathbb{E} \left[\left(\sum_{i=1}^n \mathbb{E}_{\Theta} [W_i (f(X_i) - f^*(X))] - \mathbb{1}_{\mathcal{E}^c} f^*(X) \right)^2 \right] \quad (6)$$

$$\geq \mathbb{E} [f^*(X)^2 \mathbb{1}_{\mathcal{E}^c}] \quad (7)$$

$$\geq \mathbb{E} [f^*(X)^2 \mathbb{P}(\mathcal{E}^c|X)]. \quad (8)$$

Besides,

$$\mathbb{P}(\mathcal{E}^c|X) = \mathbb{P}(N_{n,\infty}(X) = 0|X) \quad (9)$$

$$= \left(1 - \frac{1}{\alpha_n n} \right)^n, \quad (10)$$

and as $\log(1 - 1/x) \geq -\frac{1}{x-1}$ for $x > 1$,

$$\left(1 - \frac{1}{\alpha_n n} \right)^n = e^{n \log(1 - \frac{1}{\alpha_n n})} \quad (11)$$

$$\geq e^{-\frac{n}{\alpha_n n - 1}}. \quad (12)$$

The above quantity does not tend to 0 when n tends to infinity. Therefore, if $\mathbb{E} [f^*(X)^2] > 0$, the infinite CRF is inconsistent.

A.2 Proofs of Section 4 (Theorem 4.1)

In this section, we prove the consistency of the infinite KeRF estimator in the interpolating regime in expectancy (Theorem 4.1). We follow the proof given in [21] and first present two of its results.

Lemma A.1. *Let $k \in \mathbb{N}$ and consider an infinite centered random forest of depth k . Then, for all $x, \mathbf{z} \in [0, 1]^d$,*

$$K_n^{cc}(x, \mathbf{z}) = \sum_{\substack{k_1, \dots, k_d \\ \sum_{\ell=1}^d k_\ell = k}} \frac{k!}{k_1! \dots k_d!} \left(\frac{1}{d} \right)^k \prod_{j=1}^d \mathbb{1}_{\lceil 2^{k_j} x_j \rceil = \lceil 2^{k_j} z_j \rceil}.$$

Theorem A.2. *From [21]. Let f be a L -Lipschitz function. Then, for all k ,*

$$\sup_{x \in [0, 1]^d} \left| \frac{\int_{[0, 1]^d} K_k^{cc}(x, \mathbf{z}) f(\mathbf{z}) d\mathbf{z}_1 \dots d\mathbf{z}_d}{\int_{[0, 1]^d} K_k^{cc}(x, \mathbf{z}) d\mathbf{z}_1 \dots d\mathbf{z}_d} - f(x) \right| \leq Ld \left(1 - \frac{1}{2d} \right)^k.$$

Proof of Theorem 4.1. Let $x \in [0, 1]^d$, $\|f^*\|_\infty = \sup_{x \in [0, 1]^d} |f^*(x)|$ and recall that

$$\tilde{m}_{\infty, n}^{cc}(x) = \frac{\sum_{i=1}^n Y_i K_k^{cc}(x, X_i)}{\sum_{i=1}^n K_k^{cc}(x, X_i)}.$$

Thus, letting

$$\begin{aligned} A_n(x) &= \frac{1}{n} \sum_{i=1}^n \left(\frac{Y_i K_k^{cc}(x, X_i)}{\mathbb{E}[K_k^{cc}(x, X)]} - \frac{\mathbb{E}[Y K_k^{cc}(x, X)]}{\mathbb{E}[K_k^{cc}(x, X)]} \right), \\ B_n(x) &= \frac{1}{n} \sum_{i=1}^n \left(\frac{K_k^{cc}(x, X_i)}{\mathbb{E}[K_k^{cc}(x, X)]} - 1 \right), \\ \text{and } M_n(x) &= \frac{\mathbb{E}[Y K_k^{cc}(x, X)]}{\mathbb{E}[K_k^{cc}(x, X)]}, \end{aligned}$$

the estimate $\tilde{m}_{\infty,n}^{cc}(x)$ can be rewritten as

$$\tilde{m}_{\infty,n}^{cc}(x) = \frac{M_n(x) + A_n(x)}{1 + B_n(x)},$$

which leads to

$$\tilde{m}_{\infty,n}^{cc}(x) - f^*(x) = \frac{M_n(x) - f^*(x) + A_n(x) - B_n(x)f^*(x)}{1 + B_n(x)}.$$

According to Theorem A.2, we have

$$\begin{aligned} |M_n(x) - f^*(x)| &= \left| \frac{\mathbb{E}[f^*(X)K_k^{cc}(x, X)]}{\mathbb{E}[K_k^{cc}(x, X)]} + \frac{\mathbb{E}[\varepsilon K_k^{cc}(x, X)]}{\mathbb{E}[K_k^{cc}(x, X)]} - f^*(x) \right| \\ &\leq \left| \frac{\mathbb{E}[f^*(X)K_k^{cc}(x, X)]}{\mathbb{E}[K_k^{cc}(x, X)]} - f^*(x) \right| \\ &\leq C \left(1 - \frac{1}{2d} \right)^k, \end{aligned}$$

where $C = Ld$. Take $\alpha \in]0, 1/2]$. Let $\mathcal{C}_\alpha(x)$ be the event on which $\{|A_n(x)|, |B_n(x)| \leq \alpha\}$. On the event $\mathcal{C}_\alpha(x)$, we have

$$\begin{aligned} |\tilde{m}_{\infty,n}^{cc}(x) - f^*(x)|^2 &\leq 8|M_n(x) - f^*(x)|^2 + 8|A_n(x) - B_n(x)f^*(x)|^2 \\ &\leq 8C^2 \left(1 - \frac{1}{2d} \right)^{2k} + 8\alpha^2(1 + \|f^*\|_\infty)^2. \end{aligned}$$

Thus,

$$\mathbb{E}[|\tilde{m}_{\infty,n}^{cc}(x) - f^*(x)|^2 \mathbf{1}_{\mathcal{C}_\alpha(x)}] \leq 8C^2 \left(1 - \frac{1}{2d} \right)^{2k} + 8\alpha^2(1 + \|f^*\|_\infty)^2. \quad (13)$$

Consequently, to find an upper bound on the rate of consistency of $\tilde{m}_{\infty,n}^{cc}$, we just need to upper bound

$$\begin{aligned} \mathbb{E} \left[|\tilde{m}_{\infty,n}^{cc}(x) - f^*(x)|^2 \mathbf{1}_{\mathcal{C}_\alpha^c(x)} \right] &\leq \mathbb{E} \left[\max_{1 \leq i \leq n} Y_i + f^*(x) \right]^2 \mathbf{1}_{\mathcal{C}_\alpha^c(x)} \\ &\quad (\text{since } \tilde{m}_{\infty,n}^{cc} \text{ is a local averaging estimate}) \\ &\leq \mathbb{E} \left[2\|m\|_\infty + \max_{1 \leq i \leq n} \varepsilon_i \right]^2 \mathbf{1}_{\mathcal{C}_\alpha^c(x)} \\ &\leq \left(\mathbb{E} \left[2\|m\|_\infty + \max_{1 \leq i \leq n} \varepsilon_i \right]^4 \mathbb{P}[\mathcal{C}_\alpha^c(x)] \right)^{1/2} \\ &\quad (\text{by Cauchy-Schwarz inequality}) \\ &\leq \left(\left(16\|m\|_\infty^4 + 8\mathbb{E} \left[\max_{1 \leq i \leq n} \varepsilon_i \right]^4 \right) \mathbb{P}[\mathcal{C}_\alpha^c(x)] \right)^{1/2}. \end{aligned}$$

Simple calculations on Gaussian tails show that one can find a constant $C' > 0$ such that for all n ,

$$\mathbb{E} \left[\max_{1 \leq i \leq n} \varepsilon_i \right]^4 \leq C' (\log n)^2.$$

Thus, there exists C'' such that, for all $n > 1$,

$$\mathbb{E} \left[|\tilde{m}_{\infty, n}^{cc}(x) - f^*(x)|^2 \mathbf{1}_{\mathcal{C}_\alpha^c(x)} \right] \leq C'' (\log n) (\mathbb{P} [\mathcal{C}_\alpha^c(x)])^{1/2}. \quad (14)$$

The last probability $\mathbb{P} [\mathcal{C}_\alpha^c(x)]$ can be upper bounded by using Chebyshev's inequality. Indeed, with respect to $A_n(x)$,

$$\begin{aligned} \mathbb{P} [|A_n(x)| > \alpha] &\leq \frac{1}{n\alpha^2} \mathbb{E} \left[\frac{Y K_k^{cc}(x, X)}{\mathbb{E} [K_k^{cc}(x, X)]} - \frac{\mathbb{E} [Y K_k^{cc}(x, X)]}{\mathbb{E} [K_k^{cc}(x, X)]} \right]^2 \\ &\leq \frac{1}{n\alpha^2} \frac{1}{(\mathbb{E} [K_k^{cc}(x, X)])^2} \mathbb{E} \left[Y^2 K_k^{cc}(x, X)^2 \right] \\ &\leq \frac{2}{n\alpha^2} \frac{1}{(\mathbb{E} [K_k^{cc}(x, X)])^2} \left(\mathbb{E} \left[f^*(X)^2 K_k^{cc}(x, X)^2 \right] \right. \\ &\quad \left. + \mathbb{E} \left[\varepsilon^2 K_k^{cc}(x, X)^2 \right] \right) \\ &\leq \frac{2(\|f^*\|_\infty^2 + \sigma^2)}{n\alpha^2} \frac{\mathbb{E} [K_k^{cc}(x, X)^2]}{(\mathbb{E} [K_k^{cc}(x, X)])^2}. \end{aligned} \quad (15)$$

Meanwhile with respect to $B_n(x)$, we obtain, still by Chebyshev's inequality,

$$\mathbb{P} [|B_n(x)| > \alpha] \leq \frac{1}{n\alpha^2} \mathbb{E} \left[\frac{K_k^{cc}(x, X_i)^2}{(\mathbb{E} [K_k^{cc}(x, X)]^2)} \right] \quad (16)$$

which matches the control made by [21]. Note that from here, the control on $\mathbb{P} [|A_n(x)| > \alpha]$ (15) and on $\mathbb{P} [|B_n(x)| > \alpha]$ (16) will depart from the work of [21].

First, we need a Lemma to upper bound $\mathbb{E} [K_k^{cc}(x, X)^2]$.

Lemma A.3. *For all k ,*

$$\mathbb{E} [K_k^{cc}(x, X)^2] \leq v_k + 2^{-\frac{k}{d}-1} + C_2 \left(\frac{2}{d} \right)^k k^{d+1/2}$$

where C_2 is a constant depending only on d and $v_k \approx C_1 / (2^k k^{(d-1)/2})$ with C_1 also a constant depending only on d .

Proof of Lemma A.3. We know that

$$\mathbb{E} [K_k^{cc}(x, X)] = \frac{1}{2^k} \geq \mathbb{E} [K_k^{cc}(x, X)^2] \geq \mathbb{E} [K_k^{cc}(x, X)]^2 = \frac{1}{2^{2k}}, \quad (17)$$

but we need a tighter upper bound on $\mathbb{E} [K_k^{cc}(x, X)^2]$. From Lemma A.1, we know that

$$\mathbb{E} [K_k^{cc}(x, X)^2] = \mathbb{E} \left[\left(\sum_{\substack{k_1, \dots, k_d \\ \sum_{j=1}^d k_j = k}} \frac{k!}{k_1! \dots k_d!} \left(\frac{1}{d} \right)^k \prod_{j=1}^d \mathbb{1}_{\lceil 2^{k_j} x_j \rceil = \lceil 2^{k_j} z_j \rceil} \right)^2 \right]. \quad (18)$$

Developing the square within the expectation, we obtain two terms, the first one being the sum of the squares:

$$A := \mathbb{E} \left[\sum_{\substack{k_1, \dots, k_d \\ \sum_{j=1}^d k_j = k}} \left(\frac{k!}{k_1! \dots k_d!} \right)^2 \left(\frac{1}{d} \right)^{2k} \prod_{j=1}^d \mathbb{1}_{\lceil 2^{k_j} x_j \rceil = \lceil 2^{k_j} X_j \rceil} \right] \quad (19)$$

$$= \sum_{\substack{k_1, \dots, k_d \\ \sum_{j=1}^d k_j = k}} \left(\frac{k!}{k_1! \dots k_d!} \right)^2 \left(\frac{1}{d} \right)^{2k} \prod_{j=1}^d \mathbb{P}(\lceil 2^{k_j} x_j \rceil = \lceil 2^{k_j} X_j \rceil). \quad (20)$$

Note that, for all j ,

$$\mathbb{P}(\lceil 2^{k_j} x_j \rceil = \lceil 2^{k_j} X_j \rceil) = \left(\frac{1}{2} \right)^{k_j},$$

and

$$\prod_{j=1}^d \left(\frac{1}{2} \right)^{k_j} = \left(\frac{1}{2} \right)^k.$$

Therefore,

$$A = \sum_{\substack{k_1, \dots, k_d \\ \sum_{j=1}^d k_j = k}} \left(\frac{k!}{k_1! \dots k_d!} \right)^2 \left(\frac{1}{d} \right)^{2k} \left(\frac{1}{2} \right)^k. \quad (21)$$

Thanks to [19], we know that

$$\sum_{\substack{k_1, \dots, k_d \\ \sum_{j=1}^d k_j = k}} \left(\frac{k!}{k_1! \dots k_d!} \right)^2 \approx \frac{d^{2k+d/2}}{k^{(d-1)/2}}. \quad (22)$$

The second term corresponds to the sum of cross-products:

$$B := \mathbb{E} \left[\sum_{\substack{(k_1, \dots, k_d) \\ \neq (l_1, \dots, l_d), \\ \sum_{j=1}^d k_j = \sum_{j=1}^d l_j = k}} \frac{k!}{k_1! \dots k_d!} \frac{k!}{l_1! \dots l_d!} \left(\frac{1}{d} \right)^{2k} \prod_{j=1}^d \mathbb{1}_{\lceil 2^{k_j} x_j \rceil = \lceil 2^{k_j} X_j \rceil} \mathbb{1}_{\lceil 2^{l_j} x_j \rceil = \lceil 2^{l_j} X_j \rceil} \right] \quad (23)$$

$$= \sum_{\substack{(k_1, \dots, k_d) \\ \neq (l_1, \dots, l_d), \\ \sum_{j=1}^d k_j = \sum_{j=1}^d l_j = k}} \frac{k!}{k_1! \dots k_d!} \frac{k!}{l_1! \dots l_d!} \left(\frac{1}{d} \right)^{2k} \mathbb{P} \left(\bigcap_{j=1}^d ((\lceil 2^{k_j} x_j \rceil = \lceil 2^{k_j} X_j \rceil) \cap (\lceil 2^{l_j} x_j \rceil = \lceil 2^{l_j} X_j \rceil)) \right).$$

A small computation yields

$$\mathbb{P} \left(\bigcap_{j=1}^d ((\lceil 2^{k_j} x_j \rceil = \lceil 2^{k_j} X_j \rceil) \cap (\lceil 2^{l_j} x_j \rceil = \lceil 2^{l_j} X_j \rceil)) \right) = \left(\frac{1}{2} \right)^{k + \sum_{j=1}^d l_j \mathbb{1}_{l_j \neq k_j}}. \quad (24)$$

Therefore,

$$B = \left(\frac{1}{d} \right)^{2k} \left(\frac{1}{2} \right)^k \sum_{\substack{(k_1, \dots, k_d) \\ \neq (l_1, \dots, l_d), \\ \sum_{j=1}^d k_j = \sum_{j=1}^d l_j = k}} \frac{k!}{k_1! \dots k_d!} \frac{k!}{l_1! \dots l_d!} \left(\frac{1}{2} \right)^{\sum_{j=1}^d l_j \mathbb{1}_{l_j \neq k_j}}. \quad (25)$$

As $d > 2$, we can write $k = qd + r$ with $(q, r) \in \mathbb{N} \times \{0, \dots, d-1\}$. Denoting $\mathcal{K}_q = \{l = (l_1, \dots, l_d) \mid \sum_{(l_1, \dots, l_d) \neq (k_1, \dots, k_d)} l_j \geq q\}$, we can write:

$$B = \left(\frac{1}{2d^2}\right)^k \sum_{\substack{(k_1, \dots, k_d) \\ \sum_{j=1}^d k_j = k}} \frac{k!}{k_1! \dots k_d!} \sum_{l \in \mathcal{K}_q} \frac{k!}{l_1! \dots l_d!} \left(\frac{1}{2}\right)^{\sum_{j=1}^d l_j \mathbb{1}_{l_j \neq k_j}} \quad (26)$$

$$+ \left(\frac{1}{2d^2}\right)^k \sum_{\substack{(k_1, \dots, k_d) \\ \sum_{j=1}^d k_j = k}} \frac{k!}{k_1! \dots k_d!} \sum_{l \notin \mathcal{K}_q} \frac{k!}{l_1! \dots l_d!} \left(\frac{1}{2}\right)^{\sum_{j=1}^d l_j \mathbb{1}_{l_j \neq k_j}} \quad (27)$$

$$= \left(\frac{1}{2d^2}\right)^k (B_1 + B_2). \quad (28)$$

Then, regarding B_1 , as we sum over $l \in \mathcal{K}_q$,

$$\frac{k!}{k_1! \dots k_d!} \frac{k!}{l_1! \dots l_d!} \left(\frac{1}{2}\right)^{\sum_{j=1}^d l_j \mathbb{1}_{l_j \neq k_j}} \leq \frac{k!}{k_1! \dots k_d!} \frac{k!}{l_1! \dots l_d!} \left(\frac{1}{2}\right)^q \quad (29)$$

$$\leq \frac{k!}{k_1! \dots k_d!} \frac{k!}{l_1! \dots l_d!} \left(\frac{1}{2}\right)^{\frac{k}{d}-1}. \quad (30)$$

Regarding B_2 , there are at most $d-1$ integers summing at most at $q-1$. Therefore for a fixed k_1, \dots, k_d , we have

$$\sum_{l \notin \mathcal{K}} \frac{k!}{l_1! \dots l_d!} \left(\frac{1}{2}\right)^{\sum_{j=1}^d l_j \mathbb{1}_{l_j \neq k_j}} \leq \sum_{l \notin \mathcal{K}} \frac{k!}{l_1! \dots l_d!}. \quad (31)$$

As a first remark, for $s \in \{2, \dots, d-2\}$, $k!/(l_{i_1}! \dots l_{i_s}!)$ is maximal when all l_{i_s} are equal. We will use Γ function verifying $\Gamma(n+1) = n!$ for all $n \in \mathbb{N}$. Using an inequality from [5], we know that

$$\frac{k!}{l_1! \dots l_d!} \leq \frac{k!}{l_{i_1}! \dots l_{i_s}!} \quad (32)$$

$$\leq \frac{k!}{\Gamma(k/s + 1)^s} \quad (33)$$

$$\leq \sqrt{2\pi} s^{s+s/2} \frac{\sqrt{k} k^k e^{-k} e^{1/12k}}{k^{\frac{s}{2}} k^k s^{-k} e^{-k} e^{-\frac{s}{6k/s+3/s}}} \quad (34)$$

$$\leq 2C_s k^{-\frac{s-1}{2}} s^k, \quad (35)$$

with C_s a constant depending only on s . Note that when we are not in \mathcal{K} , we can choose s k_j s such that their sum is greater than $k - q + 1$. For $l \notin \mathcal{K}$, we denote $\mathcal{K}_l = \{l = (l'_1, \dots, l'_{d-s}) \mid l_j \neq k_j\}$. We obtain

$$B_2 = \sum_{p=2}^{q-1} \sum_{s=2}^{d-2} \sum_{\substack{(k_1, \dots, k_d) \\ \sum_{i=1}^s k_{j_i} = k-p \\ \sum_{i=1}^d k_i = k}} \frac{k!}{k_1! \dots k_d!} \sum_{\substack{l' \in \mathcal{K}_l \\ l_{j_1} = k_{j_1}, \dots, l_{j_s} = k_{j_s} \\ \text{fixed} \\ \sum_{i=1}^d l_i = k}} \frac{k!}{l_1! \dots l_d!} \quad (36)$$

$$\leq \sum_{p=2}^{q-1} \sum_{s=2}^{d-2} \sum_{\substack{(k_1, \dots, k_d) \\ \sum_{i=1}^s k_{j_i} = k-p \\ \sum_{i=1}^d k_i = k}} \frac{k!}{k_1! \dots k_d!} \sum_{\substack{l' \in \mathcal{K}_l \\ l_{j_1} = k_{j_1}, \dots, l_{j_s} = k_{j_s} \\ \text{fixed} \\ \sum_{i=1}^d l_i = k}} 2C_s k^{-\frac{s-1}{2}} s^k. \quad (37)$$

The number of terms in the third sum over the d-uplet with s elements being fixed equals

$$\binom{d}{s} \binom{(p-1) + d - s - 1}{p-1} \quad (38)$$

and is maximum for $p = q - 1$. Therefore,

$$B_2 \leq \sum_{p=2}^{q-1} \sum_{s=2}^{d-2} \sum_{\substack{(k_1, \dots, k_d) \\ \sum_{i=1}^s k_{j_i} = k-p \\ \sum_{i=1}^d k_i = k}} \frac{k!}{k_1! \dots k_d!} C'_s \frac{(q+d-s-3)!}{(q-2)!} k^{-\frac{s-1}{2}} s^k, \quad (39)$$

with $C'_s > 0$ a constant depending only on d . Recall that $q = \lfloor k/d \rfloor$. Note that $\frac{(q+d-s-2)!}{(q-1)!}$ is in $O(q^{d-s-2})$. The maximal term of the previous sum is therefore reached for $s = 2$. Overall, we find

$$B_2 \leq \sum_{p=2}^{q-1} \sum_{s=2}^{d-2} \sum_{\substack{(k_1, \dots, k_d) \\ \sum_{i=1}^s k_{j_i} = k-p \\ \sum_{i=1}^d k_i = k}} \frac{k!}{k_1! \dots k_d!} C_2 \cdot k^d \cdot k^{-1/2} \cdot 2^k \quad (40)$$

$$= \sum_{\substack{(k_1, \dots, k_d) \\ \sum_{i=1}^d k_i = k}} \frac{k!}{k_1! \dots k_d!} C_2 \cdot k^d \cdot k^{-1/2} \cdot 2^k, \quad (41)$$

with $C_2 > 0$ a constant depending only on d .

Finally, as

$$\sum_{\substack{k_1, \dots, k_d \\ \sum_{j=1}^d k_j = k}} \left(\frac{k!}{k_1! \dots k_d!} \right) = d^k,$$

we obtain

$$B_2 \leq C_2 \cdot (2d)^k \cdot \sqrt{k} \cdot k^d. \quad (42)$$

□

Using the previous Lemma, we have

$$\mathbb{P}(|A_n(x)| > \alpha) \leq 2M_1^2 \frac{2^k}{n\alpha^2} \left(v_k + 2^{-\frac{k}{d}-1} + C_2 \left(\frac{2}{d} \right)^k k^{d+1/2} \right), \quad (43)$$

where $v_k \approx C_d/(k^{(d-1)/2})$, and

$$\mathbb{P}(|B_n(x)| > \alpha) \leq \frac{2^k}{n\alpha^2} \left(v_k + 2^{-\frac{k}{d}-1} + C_2 \left(\frac{2}{d} \right)^k k^{d+1/2} \right).$$

Thus, the probability of $\mathcal{C}_\alpha(x)$ is given by

$$\begin{aligned} \mathbb{P}[\mathcal{C}_\alpha(x)] &\geq 1 - \mathbb{P}(|A_n(x)| \geq \alpha) - \mathbb{P}(|B_n(x)| \geq \alpha) \\ &\geq 1 - \left(\frac{2^k}{n} \frac{2M_1^2}{\alpha^2} + \frac{2^k}{n\alpha^2} \right) \left(v_k + 2^{-\frac{k}{d}-1} + C_2 \left(\frac{2}{d} \right)^k k^{d+1/2} \right). \end{aligned}$$

Consequently, according to inequality (14), we obtain

$$\mathbb{E} \left[|\tilde{m}_{\infty, n}^{cc}(x) - f^*(x)|^2 \mathbb{1}_{\mathcal{C}_\alpha^c(x)} \right] \leq C_2 (\log n) \left(\frac{2^k}{n} \frac{2M_1^2}{\alpha^2} + \frac{2^k}{n\alpha^2} \right)^{1/2} \left(v_k + 2^{-\frac{k}{d}-1} + C_2 \left(\frac{2}{d} \right)^k k^{d+1/2} \right)^{1/2}.$$

Then using inequality (13),

$$\begin{aligned}
& \mathbb{E} \left[\tilde{m}_{\infty,n}^{cc}(x) - f^*(x) \right]^2 \\
& \leq \mathbb{E} \left[|\tilde{m}_{\infty,n}^{cc}(x) - f^*(x)|^2 \mathbf{1}_{C_\alpha(x)} \right] + \mathbb{E} \left[|\tilde{m}_{\infty,n}^{cc}(x) - f^*(x)|^2 \mathbf{1}_{C_\alpha^c(x)} \right] \\
& \leq 8C_1^2 \left(1 - \frac{1}{2d} \right)^{2k} + 8\alpha^2(1 + \|m\|_\infty)^2 \\
& \quad + C_2(\log n) \left(\frac{2^k}{n} \frac{2M_1^2}{\alpha^2} + \frac{2^k}{n\alpha^2} \right)^{1/2} \left(v_k + 2^{-\frac{k}{d}-1} + C_2 \left(\frac{2}{d} \right)^k k^{d+1/2} \right)^{1/2}.
\end{aligned}$$

Optimizing the right hand side in α

($\alpha^3 = C_2(\log n) \left(\frac{2^k}{n} 2M_1^2 + \frac{2^k}{n} \right)^{1/2} \left(v_k + 2^{-\frac{k}{d}-1} + C_2 \left(\frac{2}{d} \right)^k k^{d+1/2} \right)^{1/2} (1 + \|m\|_\infty)^{-2}/16$), we get

$$\begin{aligned}
& \mathbb{E} \left[\tilde{m}_{\infty,n}^{cc}(x) - f^*(x) \right]^2 \\
& \leq 8C_1^2 \left(1 - \frac{1}{2d} \right)^{2k} + C_3(\log n)^{2/3} \left(\frac{2^k}{n} 2M_1^2 + \frac{2^k}{n} \right)^{1/3} \left(v_k + 2^{-\frac{k}{d}-1} + C_2 \left(\frac{2}{d} \right)^k k^{d+1/2} \right)^{1/3}.
\end{aligned}$$

for some constant $C_3 > 0$. Choosing $k_n = \lfloor \log_2(n) \rfloor$, we obtain:

$$\mathbb{E} \left[\tilde{m}_{\infty,n}^{cc}(x) - f^*(x) \right]^2 \tag{44}$$

$$\leq C_d n^{2\log(1-\frac{1}{d})} + C_d (\log n)^{2/3} \left(w_n + \frac{n^{-1/2d}}{2} + n^{-\log_2(d-2)} (\log n)^{d+1/2} \right)^{1/3}, \tag{45}$$

with $C_d > 0$ and $w_n \approx \log(n)^{-(d-1)/2}$. Finally,

$$\begin{aligned}
\mathbb{E} \left[\tilde{m}_{\infty,n}^{cc}(x) - f^*(x) \right]^2 & \leq C_d \left(\log(n)^2 w_n + \frac{\log(n)^2 n^{-1/d}}{2} + n^{-\log_2(d-2)} (\log n)^{d+5/2} \right)^{1/3} \\
& \quad + C_d n^{2\log(1-\frac{1}{2d})}.
\end{aligned}$$

□

A.3 Proofs of section 5

A.3.1 Proof of Lemma 5.1

To begin with, we have

$$\mathbb{P}(k_n(X) \geq k) = \mathbb{P} \left(\bigcap_{i=1}^{k-1} N_{i,\Theta}(X) \geq 2 \right) \tag{46}$$

$$= \mathbb{P}(N_{1,\Theta} \geq 2) \prod_{i=2}^{k-1} \mathbb{P}(N_{i,\Theta}(X) \geq 2 | N_{i-1,\Theta}(X) \geq 2) \tag{47}$$

$$= \mathbb{P}(N_{k-1,\Theta}(X) \geq 2) \tag{48}$$

$$= \mathbb{E} [\mathbb{P}(N_{k-1,\Theta}(X) \geq 2 | X)] \tag{49}$$

$$= 1 - \left(1 - \frac{1}{2^{k-1}} \right)^n - \frac{n}{2^{k-1}} \left(1 - \frac{1}{2^{k-1}} \right)^{n-1}. \tag{50}$$

Studying the right-hand side of equality (50) with $k = (1 - \log^{-\alpha}(n)) \log_2(n)$ and using the inequalities

$$\exp\left(-\frac{n}{2^k - 1}\right) \leq \exp\left(n \log\left(1 - \frac{1}{2^k}\right)\right) \leq \exp\left(-\frac{n}{2^k}\right)$$

yields the result.

A.3.2 Proof of Lemma 5.3

Given a single tree built with Θ_1 , a random point x , its depth $k_n(x)$ and $A_{n,-1} := A_{n,-1}(x, \Theta_1)$ the node preceding the leaf $A_n(x, \Theta_1)$, two configurations lead to x falling into an empty cell :

1. All the X_i 's are in the leaf diametrically opposite to the leaf $A_n(x)$ within the cell $A_{n,-1}(x)$ (see point X on Figure 6).
2. At least one of the X_i 's falls in an adjacent leaf of $A_n(x)$ (along any feature) within $A_{n,-1}(x)$ (see point X' on Figure 6).

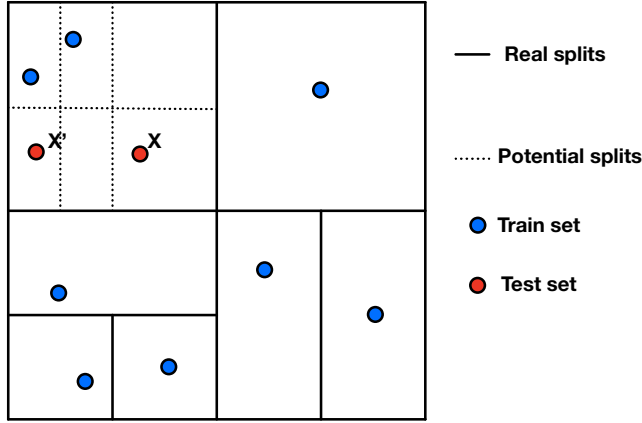


Figure 6: Illustration of situations 1 and 2.

Situation 1. could lead to x falling in an empty leaf for all tree, whereas in situation 2., a tree could produce a non-empty cell containing x with a probability greater than 0 by choosing a different feature to cut over in node $A_{n,-1}$. These two situations are illustrated on Figure 6: for this tree, in the node $A_{n,-1}$, X can only fall into an empty cell for all trees whereas the point X' could fall in a non-empty cell if the randomly selected next split is vertical. Therefore, in situation 2., the probability of x falling in an empty cell in the infinite forest is 0.

Call \mathcal{E}_M the event “ $N_n(x, \Theta_M) = 0$ ”. We denote $S_1(\Theta_M)$ the event “there exists a tree Θ_j in Θ_M for which all the X_i 's are in the leaf diametrically opposite to the leaf $A_n(x)$ within the cell $A_{n,-1}(x)$ ” and $S_2(\Theta_M)$ the event “for all trees Θ_j of Θ_M , at least one of the X_i 's falls in an adjacent leaf of $A_n(x)$ (along any feature) within $A_{n,-1}(x)$ ”.

Then,

$$\mathbb{P}(\mathcal{E}_M) = \mathbb{P}((N_n(X, \Theta_M) = 0) \cap S_1(\Theta_M)) + \mathbb{P}((N_n(X, \Theta_M) = 0) \cap S_1^c(\Theta_M)) \quad (51)$$

$$= \mathbb{P}((N_n(X, \Theta_M) = 0) \cap S_1(\Theta_M)) + \mathbb{P}((N_n(X, \Theta_M) = 0) \cap S_2(\Theta_M)) \quad (52)$$

$$\leq M\mathbb{P}(S_1(\Theta_1)) + \mathbb{P}(S_2(\Theta_M)). \quad (53)$$

We use the following Lemma to compute $\mathbb{P}(S_1(\Theta_1))$:

Lemma A.4. *One has*

$$\mathbb{P}(S_1(\Theta_1)) \leq \frac{4}{2n - 1}.$$

Proof. Recall that the event $S_1(\Theta_1)$ happens when all X_i 's are in the leaf $A_{n,-1,OD}(X)$ Diametrically Opposite to the leaf $A_n(x)$ within the cell $A_{n,-1}(x)$.

$$\begin{aligned}
\mathbb{P}(S_1(\Theta_1)) &\leq \binom{2^d}{1} \cdot \mathbb{E} \left[\mathbb{E} \left[\mathbb{P} \left(\left(X_{i_1}, \dots, X_{i_{N_n(A_{n,-1})}} \right) \in A_{n,-1,OD}(X) \right. \right. \right. \\
&\quad \left. \left. \left. \cap (X \in A_n(X) \mid N_n(A_{n,-1})) \right) \mid A_{n,-1} \right] \right] \\
&= 2^d \cdot \mathbb{E} \left[\mathbb{E} \left[\frac{\mu(A_{n,-1})}{2^d} \left(\frac{\mu(A_{n,-1})}{2^d} \right)^{N_n(A_{n,-1})} \mid A_{n,-1} \right] \right] \\
&= \mathbb{E} \left[\frac{1}{2^{k_n(x)-1}} \left(1 - \frac{1}{2^{k_n(x)-1}} + \frac{1}{2^{k_n(x)+d-1}} \cdot \frac{1}{2^{k_n(x)-1}} \right)^n \right] \\
&\leq 2 \cdot \mathbb{E} \left[\frac{1}{2^{k_n(x)}} \left(1 - \frac{1}{2^{k_n(x)}} + \frac{1}{2^{2k_n(x)}} \right)^n \right],
\end{aligned}$$

as soon as $d \geq 2$. We introduce the function $g \in C^1([1, \infty))$ defined as

$$g : z \rightarrow \frac{1}{z} \left(1 - \frac{1}{z} + \frac{1}{z^2} \right)^n.$$

Let $z \geq 1$, we have

$$g'(z) = \frac{\left(\frac{1}{z^2} - \frac{1}{z} + 1\right)^n (n(z-2) - z^2 + z - 1)}{z^2(z^2 - z + 1)}.$$

Consequently,

$$\begin{aligned}
g'(z) \geq 0 &\iff -z^2 + z(n+1) - (2n+1) \geq 0 \\
&\iff z \leq \frac{(n+1) + \sqrt{(n+1)^2 - 4(2n+1)}}{2} := r_n^*
\end{aligned}$$

with $n \geq 6$. Note that g is non-decreasing over $[1, r_n^*]$ and non-increasing over $[r_n^*, \infty)$, its maximum is reached at $z = r_n^*$. Finally,

$$\begin{aligned}
\mathbb{P}(\mathcal{E}) &\leq \frac{4}{n+1 + \sqrt{\Delta_n}} \left(1 - \frac{2}{n+1 + \sqrt{\Delta_n}} + \frac{4}{(n+1 + \sqrt{\Delta_n})^2} \right)^n \\
&\leq \frac{4}{2n-1}.
\end{aligned}$$

□

Besides,

$$\mathbb{P}(S_2(\Theta_M)) = \mathbb{E}[\mathbb{P}(S_2(\Theta_M) \mid X, \mathcal{D}_n)] \tag{54}$$

$$= \mathbb{E}[\mathbb{P}(S_2(\Theta_1) \mid X, \mathcal{D}_n)^M]. \tag{55}$$

as the trees are built independently conditional on \mathcal{D}_n . Furthermore, note that the probability is taken over Θ_1 . Therefore for a given x , for any configuration of the dataset, if there exists a tree Θ such that $S_2(\Theta) \mid \mathcal{D}_n$ can be realized, it means that there is a cut that leads x to fall into an empty cell of an adjacent non-empty one. As a matter of fact, there also exists a tree Θ' such that $S_2(\Theta) \mid \mathcal{D}_n$ does not happen, meaning that there exists another cut such that x does not end in an empty cell. This last cut happens with probability at least equal to $1/d$. Consequently,

$$\mathbb{P}(S_2(\Theta_1) \mid X, \mathcal{D}_n) \leq 1 - \frac{1}{d}. \tag{56}$$

Finally,

$$\mathbb{P}(\mathcal{E}_M) \leq \frac{4M}{2n-1} + \left(1 - \frac{1}{d}\right)^M. \quad (57)$$

A.3.3 Proof of theorem 5.2

We upper bound the risk by classically bounding the approximation error (the estimation error is 0 in the noiseless setting). We follow the sketch of proof given by [14] when bounding the risk of a centered random forest. First note that as the X_i s are uniform and i.i.d., by symmetry, after averaging w.r.t the data, the probability to choose a given feature j for any node is always $1/d$ as no feature has more chance to produce an empty leaf than others.

Let $m_n(X)$ be the infinite adaptive centered RF and $\bar{m}_n(X) = \mathbb{E}[m_n(X)|X, X_1, \dots, X_n]$. We denote $k_n(X)$ the effective depth of the leaf containing X and k_n the maximum depth of each tree. We choose $k_n \geq n$ as we want to interpolate. We begin by bounding the approximation error (which ends the proof of consistency in a noiseless setting). We define

$$W_i := \frac{\mathbb{1}_{X_i \in A_n(x, \Theta_j)} \mathbb{1}_{N_n(x, \Theta_j) > 0}}{N_n(x, \Theta_j)}.$$

The new estimator writes

$$m_{M,n}(x, \Theta_M) = \frac{\mathbb{1}_{N_n(x, \Theta_M) > 0}}{N_n(x, \Theta_M)} \sum_{j=1}^M \sum_{i=1}^n Y_i \frac{\mathbb{1}_{x \in A_n(X_i, \Theta_j)}}{N_n(x, \Theta_j)} \mathbb{1}_{N_n(x, \Theta_j) > 0} \quad (58)$$

$$= \frac{\mathbb{1}_{N_n(x, \Theta_M) > 0}}{N_n(x, \Theta_M)} \sum_{j=1}^M \sum_{i=1}^n Y_i W_{ij} \quad (59)$$

where $W_{ij} = \frac{\mathbb{1}_{x \in A_n(X_i, \Theta_j)}}{N_n(x, \Theta_j)} \mathbb{1}_{N_n(x, \Theta_j) > 0}$. We have

$$\mathbb{E} \left[(\bar{m}_n(X) - f^*(X))^2 \right] \quad (60)$$

$$= \mathbb{E} \left[\left(\frac{\mathbb{1}_{N_n(X, \Theta_M) > 0}}{N_n(X, \Theta_M)} \sum_{j=1}^M \sum_{i=1}^n Y_i W_{ij} - f^*(X) \right)^2 \right] \quad (61)$$

$$= \mathbb{E} \left[\left(\frac{\mathbb{1}_{N_n(X, \Theta_M) > 0}}{N_n(X, \Theta_M)} \sum_{j=1}^M \sum_{i=1}^n Y_i W_{ij} - (\mathbb{1}_{N_n(X, \Theta_M) > 0} + \mathbb{1}_{N_n(X, \Theta_M) = 0}) f^*(X) \right)^2 \right] \quad (62)$$

$$\leq 2\mathbb{E} \left[\mathbb{1}_{N_n(X, \Theta_M) > 0} \left(\frac{1}{N_n(X, \Theta_M)} \sum_{j=1}^M \sum_{i=1}^n Y_i W_{ij} - f^*(X) \right)^2 \right] \quad (63)$$

$$+ 2\mathbb{E} \left[\mathbb{1}_{N_n(X, \Theta_M) = 0} f^{*2}(X) \right]. \quad (64)$$

The right-hand term of the above sum verifies

$$\mathbb{E} \left[\mathbb{1}_{N_n(X, \Theta_M) = 0} f^{*2}(X) \right] \leq \|f^*\|_\infty^2 \mathbb{P}(N_n(X, \Theta_M) = 0). \quad (65)$$

It can be controlled by applying Lemma 5.3 stating that

$$\mathbb{P}(N_n(X, \Theta_M) = 0) \leq \frac{4M}{2n-1} + \left(1 - \frac{1}{d}\right)^M,$$

from which we immediately deduce that

$$\mathbb{E} [\mathbf{1}_{N_n(X, \Theta_M)=0} f^*(X)^2] \leq \|f^*\|_\infty^2 \left(\frac{4M}{2n-1} + \left(1 - \frac{1}{d}\right)^M \right).$$

Regarding the left-hand term of Line (64),

$$\mathbb{E} \left[\mathbf{1}_{N_n(X, \Theta_M) > 0} \left(\frac{1}{N_n(X, \Theta_M)} \sum_{j=1}^M \sum_{i=1}^n Y_i W_{ij} - f^*(X) \right)^2 \right] \quad (66)$$

$$= \mathbb{E} \left[\mathbf{1}_{N_n(X, \Theta_M) > 0} \left(\frac{1}{N_n(X, \Theta_M)} \sum_{j=1}^M \sum_{i=1}^n (Y_i - f^*(X)) W_{ij} \right)^2 \right] \quad (67)$$

$$\leq \mathbb{E} \left[\left(\frac{1}{N_n(X, \Theta_M)} \sum_{j=1}^M \sum_{i=1}^n (Y_i - f^*(X)) W_{ij} \right)^2 \right] \quad (68)$$

$$\leq \sum_{j=1}^M \mathbb{E} \left[\frac{1}{N_n(X, \Theta_M)} \left(\sum_{i=1}^n (Y_i - f^*(X)) W_{ij} \right)^2 \right] \quad (69)$$

$$= \mathbb{E} \left[\frac{M}{N_n(X, \Theta_M)} \left(\sum_{i=1}^n (Y_i - f^*(X)) W_{i1} \right)^2 \right] \quad (70)$$

where the penultimate line comes from the application of Cauchy-Schwarz inequality. As we are in a noiseless setting, $Y_i = f^*(X_i)$ for all i . To upper bound the above term, note that

$$|f(X_i) - f^*(X)| \leq \sum_{j=1}^d \|\partial_j f^*\|_\infty |X_i^{(j)} - X^{(j)}| \quad (71)$$

and therefore

$$W_{i1} |f(X_i) - f^*(X)| \leq W_{i1} \sum_{j=1}^d \|\partial_j f^*\|_\infty |b_j - a_j| \quad (72)$$

where the cell $A_n(X, \Theta_j) = \prod_j [a_j, b_j]$. Thus,

$$\sum_{i=1}^n W_{i1} |f(X_i) - f^*(X)| \leq \sum_{i=1}^n W_{i1} \sum_{j=1}^d \|\partial_j f^*\|_\infty |b_j - a_j| \quad (73)$$

$$\leq \sum_{j=1}^d \|\partial_j f^*\|_\infty |b_j - a_j|. \quad (74)$$

Consequently,

$$\mathbb{E} \left[\frac{M}{N_n(X, \Theta_M)} \left(\sum_{i=1}^n (Y_i - f^*(X)) W_{i1} \right)^2 \right] \quad (75)$$

$$\leq \mathbb{E} \left[\frac{M}{N_n(X, \Theta_M)} \left(\sum_{j=1}^d \|\partial_j f^*\|_\infty |b_j - a_j| \right)^2 \right] \quad (76)$$

$$\leq Md \|\partial f^*\|_\infty^2 \sum_{j=1}^d \mathbb{E} [(b_j - a_j)^2], \quad (77)$$

where $\|\partial f^*\|_\infty = \max_j \|\partial_j f^*\|_\infty$. For al $j \in \{1, \dots, d\}$, let $K_j(X)$ be the number of splits made on feature j to produce the cell containing X . Note that, by definition of AdaCRF,

$$\mathbb{E} [(b_j - a_j)^2] = \mathbb{E} [2^{-2K_j(X)}] \quad (78)$$

$$= \mathbb{E} \left[\mathbb{E} [2^{-2K_j(X)} | X] \right] \quad (79)$$

$$\leq \mathbb{E} \left[\mathbb{E} [2^{-2K_j(X)} \mathbf{1}_{k_n(X) \geq (1-\varepsilon_n) \log_2(n)+1} | X] \right] + \mathbb{P}(k_n(X) < (1-\varepsilon_n) \log_2(n) + 1), \quad (80)$$

where ε_n is a positive sequence to be chosen later. The behavior of k_n is controlled in Lemma 5.1, which leads to

$$\mathbb{P}(k_n(X) \geq (1-\varepsilon_n) \log_2(n) + 1) \geq 1 - \left(1 - \frac{1}{n^{1-\varepsilon_n}}\right)^n - \frac{n}{n^{1-\varepsilon_n}} \left(1 - \frac{1}{n^{1-\varepsilon_n}}\right)^{n-1} \quad (81)$$

$$\geq 1 - p_n, \quad (82)$$

with $p_n = e^{-n\varepsilon_n} + n^{\varepsilon_n} e^{-n\varepsilon_n}$. The last inequality is obtained from the fact that $e^{n \log(1-1/x)} \leq e^{-n/x}$ for all $x > 0$. Besides, the random variable $K_j(X)$ is conditionally distributed as a binomial distribution of parameters $(k_n(X), 1/d)$. Consequently,

$$\mathbb{E} [(b_j - a_j)^2] \leq \mathbb{E} \left[\mathbb{E} [2^{-2K_j(X)} \mathbf{1}_{k_n(X) \geq (1-\varepsilon_n) \log_2(n)+1} | X] \right] + p_n \quad (83)$$

$$\leq \left(1 - \frac{3}{4d}\right)^{(1-\varepsilon_n) \log_2(n)+1} + p_n \quad (84)$$

$$\leq n^{(1-\varepsilon_n) \log(1-3/4d)/\log 2} + e^{-n\varepsilon_n} + n^{\varepsilon_n} e^{-n\varepsilon_n}, \quad (85)$$

where the penultimate inequality comes from the moment-generating function of the binomial distribution. A proper choice of $\varepsilon_n = (\log(n))^{-\alpha}$ for $\alpha \in (-1, 0]$, leads to, for all n large enough,

$$\mathbb{E} [(b_j - a_j)^2] \leq 3n^{\log(1-3/4d)/\log 2}. \quad (86)$$

Finally, the approximation error satisfies, for all n large enough,

$$\mathbb{E} [(\bar{m}_n(X) - f^*(X))^2] \leq 3Md^2 \|\partial f^*\|_\infty^2 n^{\log(1-3/4d)/\log 2} + \|f^*\|_\infty^2 \left(\frac{4M}{2n-1} + \left(1 - \frac{1}{d}\right)^M \right).$$

Now, choosing

$$M = \frac{\log(1-3/4d)}{\log(1-\frac{1}{d})} \log_2(n), \quad (87)$$

we obtain, for all n large enough,

$$\mathbb{E} [(\bar{m}_n(X) - f^*(X))^2] \leq C_d \log(n) n^{\log(1-3/4d)/\log 2}.$$

In the noiseless setting, the estimation error equals 0, which ends the proof.

A.3.4 Proof of Proposition 5.5

The computation is similar to the computation of the volume of the minimal interpolation zone of Breiman RF in A.4. The main difference lies on the fact that the volume of each leaf is entirely determined by the depth of the leaf. We begin with a one-dimensional analysis. Let Z_1, \dots, Z_n be i.i.d. according to a uniform distribution on $[0, 1]$. Then, we can apply the reasoning of Lemma 5.1 in one dimension to write

$$\mathbb{P}(k_n(Z_1) \leq k) = \left(1 - \frac{1}{2^{k-1}}\right)^{n-1} \quad (88)$$

and therefore

$$\mathbb{E}[\mu(A_n(Z_1))] = \mathbb{E}\left[\frac{1}{2^{k_n(Z_1)}}\right]. \quad (89)$$

Let ζ be a random variable with CDF defined as

$$F_\zeta(x) : x \in \mathbb{R} \rightarrow \left(1 - \frac{1}{2^x}\right)^{n-1} \mathbf{1}_{x \geq 1}.$$

We immediately obtain that for all x , $F_\zeta(x) \geq F_{k_n(X_1)}(x)$. As the function $x \rightarrow 2^{-x}$ is non-increasing, for all x ,

$$F_{2^{-\zeta}}(x) \leq F_{2^{-k_n(X_1)}}(x).$$

Writing $E[Z_1] = \int(1 - F_{\zeta_1})$, we see that $F_{\zeta_1} \leq F_{\zeta_2}$ implies

$$E[\zeta_1] \geq E[\zeta_2].$$

Therefore,

$$\mathbb{E}\left[2^{-k_n(X_1)}\right] \leq \mathbb{E}\left[2^{-Z}\right]. \quad (90)$$

We use the definition of Riemann-Stieltjes integrals and an integration by parts to write the following:

$$\mathbb{E}\left[2^{-k_n(X_1)}\right] \leq \mathbb{E}\left[2^{-Z}\right] \quad (91)$$

$$= \int_{-\infty}^{\infty} 2^{-x} dF_Z(x) \quad (92)$$

$$= \int_{-\infty}^{\infty} \log 2 \cdot 2^{-x} F_Z(x) dx \quad (93)$$

$$\leq 2 \int_1^{\infty} 2^{-x} \left(1 - \frac{1}{2^x}\right)^{n-1} dx \quad (94)$$

Applying the change of variable $u = 2^{-x}$ immediately yields

$$\mathbb{E}\left[2^{-k_n(X_1)}\right] \leq \frac{2}{\log 2} \int_0^{1/2} u(1-u)^{n-1} du \quad (95)$$

$$= \frac{2}{\log 2} \frac{1 - 2^{-(n+1)}(n-2)}{n(n+1)}. \quad (96)$$

Finally we obtain

$$\mathbb{E}[\mu(A_n(Z_1))] = \mathbb{E}\left[\frac{1}{2^{k_n(Z_1)}}\right] \quad (97)$$

$$\leq \frac{2}{\log 2} \frac{1 - 2^{-n}}{n}. \quad (98)$$

Applying the cartesian product along all dimensions yields the result.

A.4 Proofs of section 6

Proof of 6.1. Before diving into the computations, let us recall two facts about Breiman RF construction. First, when a CART cuts between two points, the cut is made at the middle of these two points. Second, assume that all the cuts are possible, i.e. that the probability of cutting between all pairs of successive points along all dimensions is strictly positive. Therefore, for a given point X_i , one can define the minimal interpolation zone $\mathcal{A}_{min, X_i} := \bigcap_{M \in \mathbb{N}, \Theta_M} (\cdot, \Theta_M) \mathcal{A}_{X_i, \Theta_M}$ around X_i . The boundaries of this area are given for each direction by the cuts between X_i and its *neighbor points* respectively to the considered direction, as illustrated on Figure 7.

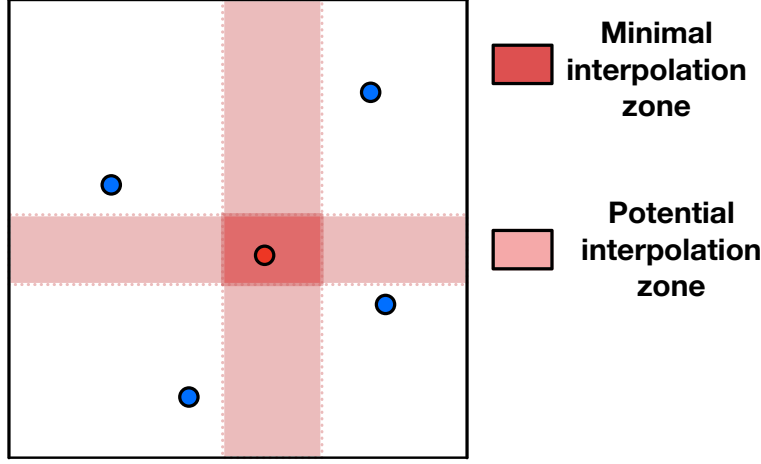


Figure 7: Different interpolation zones of a data point (in red).

1. The interpolation zone is the union of n interpolation zones, each one containing a single X_i . We denote $\mathcal{A}(m_{M,n}(\cdot, \Theta_M)) = \mathcal{A}_{X_1, \Theta_M} \cup \dots \cup \mathcal{A}_{X_n, \Theta_M}$ with $\mathcal{A}_{X_i, \Theta_M} = \{x \in [0, 1]^d, m_{M,n}(x, \Theta_M) = Y_i\}$. We begin with a one-dimensional analysis. We denote $X_i^{(j)}$ the j -th feature of X_i , for all $j \in \{1, \dots, d\}$ and $i \in \{1, \dots, n\}$ and we focus on the first variable $X^{(1)}$. As X_1, \dots, X_n are i.i.d. and follow a uniform distribution over $[0, 1]^d$, $X_1^{(1)}, \dots, X_n^{(1)}$ are i.i.d. and uniformly distributed on $[0, 1]$. For the ease of notation, we define $Z_1 := X_1^{(1)}, \dots, Z_n := X_n^{(1)}$. Let $x = Z_n$. The length (volume) of \mathcal{A}_{min, Z_n} restricted to the first dimension is simply given by the sum of the distance from x to its closest point on the left side and to its closest point on the right side (divided by 2 as the cut are made in the middle of two points). Therefore,

$$\mu(\mathcal{A}_{min, x}) = \frac{1}{2} \left(x - \max_{\{Z_i, Z_i \leq x\} \cup \{0\}} Z_i + \min_{\{Z_i, Z_i \geq x\} \cup \{1\}} Z_i - x \right) \quad (99)$$

All computations are made conditionally on x . Denoting N_x the cardinal of the set $\{Z_i : Z_i \leq x \text{ with } 1 \leq i < n\}$, we have for any $t \in [0, x/2)$,

$$\begin{aligned} & \mathbb{P} \left(\frac{1}{2} \left(x - \max_{\{Z_i, Z_i \leq x\} \cup \{0\}} Z_i \right) \leq t \mid x \right) \\ &= 1 - \mathbb{P} \left(\max_{\{Z_i, Z_i \leq x\} \cup \{0\}} Z_i < x - 2t \mid x \right) \\ &= 1 - \mathbb{E} \left[\mathbb{E} \left[\mathbb{P} \left((Z_{i_1} < x - 2t) \cap \dots \cap (Z_{i_{N_x}} < x - 2t) \mid N_x, Z_{i_1} \leq x, \dots, Z_{i_{N_x}} \leq x \right) \mid x \right] \right] \\ &= 1 - \mathbb{E} \left[(Z_1 < x - 2t \mid Z_1 \leq x)^{N_x} \mid x \right] \\ &= 1 - \sum_{k=0}^{n-1} \mathbb{P}(N_x = k \mid x) \mathbb{P}(Z_1 < x - 2t \mid Z_1 \leq x)^k \\ &= 1 - \sum_{k=0}^{n-1} \mathbb{P}(N_x = k \mid x) \left(\frac{x - 2t}{x} \right)^k \\ &= 1 - \left((1 - x) + x \left(\frac{x - 2t}{x} \right) \right)^{n-1} \\ &= 1 - (1 - 2t)^{n-1} \end{aligned}$$

where the penultimate equality is obtained by noticing that N_x is a binomial of parameters $(n - 1, x)$ and computing its probability-generating function.

So for all $t \geq 0$,

$$\mathbb{P} \left(\frac{1}{2} \left(x - \max_{\{Z_i, Z_i \leq x\} \cup \{0\}} Z_i \right) \leq t \mid x \right) = 1 - (1 - 2t)^{n-1} \mathbf{1}_{t < x/2}$$

By symmetry,

$$\mathbb{P}\left(\frac{1}{2}\left(\min_{\{Z_i, Z_i \geq x\} \cup \{1\}} Z_i - x\right) \leq t|x\right) = 1 - (1 - 2t)^{n-1} \mathbf{1}_{t > (1-x)/2}$$

Overall, using the fact that for any variable Z with cumulative function F_Z , $\mathbb{E}[Z] = \int(1 - F_Z)$, we have

$$\begin{aligned} \mathbb{E}[\mu(\mathcal{A}_{min,x})|x] &= \int_0^{x/2} (1 - 2u)^{n-1} du + \int_0^{(1-x)/2} (1 - 2u)^{n-1} du \\ &= \frac{1}{2n} (2 - (1-x)^n - x^n) \\ &\leq \frac{1}{n} \left(1 - \frac{1}{2^n}\right) \end{aligned}$$

Now, as X_1, \dots, X_n are i.i.d. and uniformly distributed over $[0, 1]^d$, for any data point $x \in [0, 1]^d$ we simply have that

$$\mathcal{A}_{min,x} = \bigtimes_{j=1}^d \mathcal{A}_{min,x^{(j)}}.$$

Therefore,

$$\mathbb{E}[\mu(\mathcal{A}_{min,x})] \leq \frac{1}{n^d} (1 - 2^{-n})^d.$$

Finally, since by definition all interpolation zones are disjoint, we have

$$\mathbb{E}[\mu(\mathcal{A}_{min})] \leq \frac{1}{n^{d-1}} (1 - 2^{-n})^d.$$

2. It is enough to notice that the minimal interpolation zone is the intersection of all the potential interpolation zones. It is reached when the forest contains all the possible cuts. Then, as the probability of any given cut appearing is strictly greater than 0 by hypothesis, the probability of its appearance in the infinite forest is one. Therefore almost surely, when M grows to infinity, the interpolation zone of the forest reaches the minimal interpolation zone.

□

B Experiment supplementary

For all experiments, we introduce the following regression models.

- **Model 1:** $d = 2$, $Y = 2X_1^2 + \exp(-X_2^2)$
- **Model 2:** $d = 8$, $Y = X_1X_2 + X_3^2 - X_4X_5 + X_6X_7 - X_8^2 + \mathcal{N}(0, 0.5)$
- **Model 3:** $d = 6$, $Y = X_1^2 + X_2^2X_3e^{-|X_4|} + X_5 - X_6 + \mathcal{N}(0, 0.5)$
- **Model 4:** $d = 5$, $Y = 1/(1 + \exp(-10 * (\sum_{i=1}^d X_i - 1/2))) + \mathcal{N}(0, 0.05)$

All the experiments are conducted using Python3. We use Scikit-learn RandomForestRegressor class to implement the Breiman RF model. We coded CRF, KeRF and AdaCRF models ourselves, mainly relying on *numpy* and *joblib* libraries for computation optimisation.

B.1 Consistency experiments

For all consistency experiments, the dataset was divided into a train dataset (80% of the data) and a test dataset (20%) of the data.

The parameters of the estimators were set as follows:

- all RF estimators have 500 *trees* to mimic the behavior of the infinite RF.
- the *max depth* parameter is set to *None* for all RF estimators, which corresponds to growing each tree until pure leaves.
- parameter *bootstrap* is set to *False* for all estimators in order preserve the interpolation property, or set to *True* when specified.
- all other parameters are set to default value for Breiman RF.

B.1.1 Consistency of Breiman RF with max-feature= 1

On Figure 8, we see that the excess risk of a Breiman RF with the max-features parameter set to 1 is decreasing towards 0 as n increases. This RF seems consistent for all models.

B.2 Interpolation experiments

B.2.1 Volume of the interpolation zone w.r.t sample size n

We plot on Figure 9 the log-volume of the interpolation zone of a Breiman RF with the max-features parameter set to $\lceil d/3 \rceil$ (the default value proposed in R `randomForest` package). The volume decreases polynomially in n but slower than when max-features= 1 (Figure 3) which is to be expected: choosing max-features= 1 should increase the diversity of the splits and therefore reduce the volume of the interpolation zone.

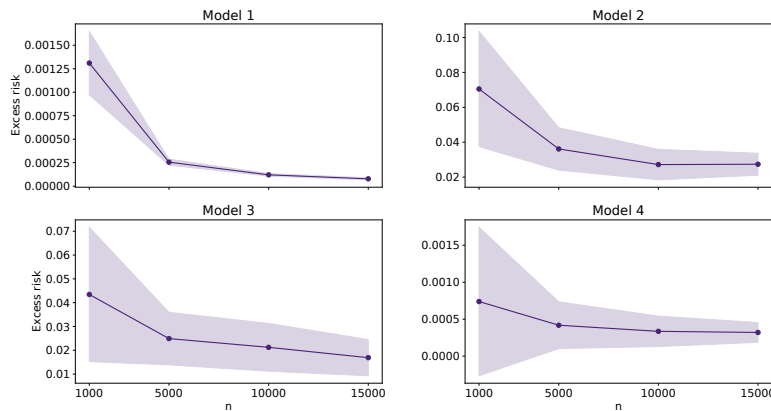


Figure 8: Consistency of Breiman RF: excess risk w.r.t sample size. RF parameters: 500 trees, max-depth set to None, max-features= 1, no bootstrap. Mean over 30 tries(dotted line) and std (filled zone).

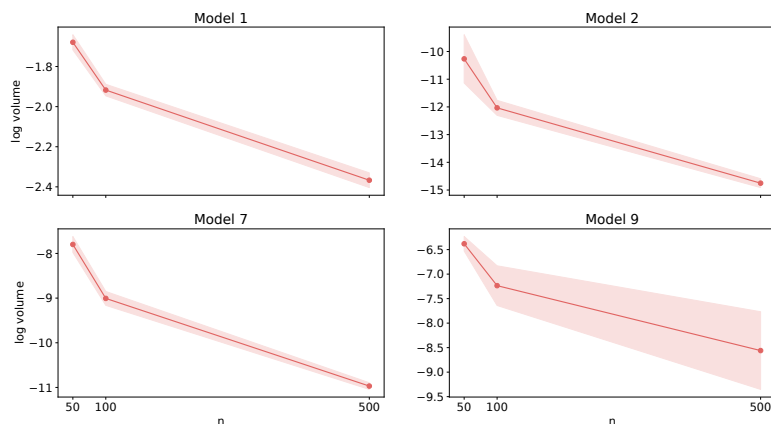


Figure 9: Log volume of Breiman RF interpolation zone w.r.t. sample size n . RF parameters: 500 trees, no bootstrap, max features = $\lceil d/3 \rceil$. Mean over 10 tries (bold line) and std (filled zone).

B.2.2 Volume of the interpolation zone w.r.t number of trees M

In this section, we empirically measure how fast decreases the volume of the interpolation zone of a Breiman RF when its number of trees M increases, and how close the interpolation zone gets from the minimal interpolation zone.

To this end, for a fixed sample size $n = 500$, we numerically evaluate the volume of the interpolation area when the number M of trees in the forest grows. This volume is anticipated to be a non-increasing function of M (for $M = 1$, note that the interpolation volume is 1, the volume of $[0, 1]^d$), but its decrease rate highly depends on the data geometry, making its theoretical evaluation difficult. The numerical results in Figure 10 show a fast decay towards zero of the interpolation volume for all models, already tiny from $M = 500$ trees. Furthermore, it seems to converge to the theoretical bound (dotted line) derived in Proposition 6.1 for an infinite RF with a max-feature parameter equal to 1.

B.2.3 Analysis of the interpolation property of Breiman RF with bootstrap

In this experiment, we try to measure how close a Breiman RF with bootstrap on is from exactly interpolating (with other parameters being 500 trees, max-depth set to None, max-features= d). To this end, we measure the

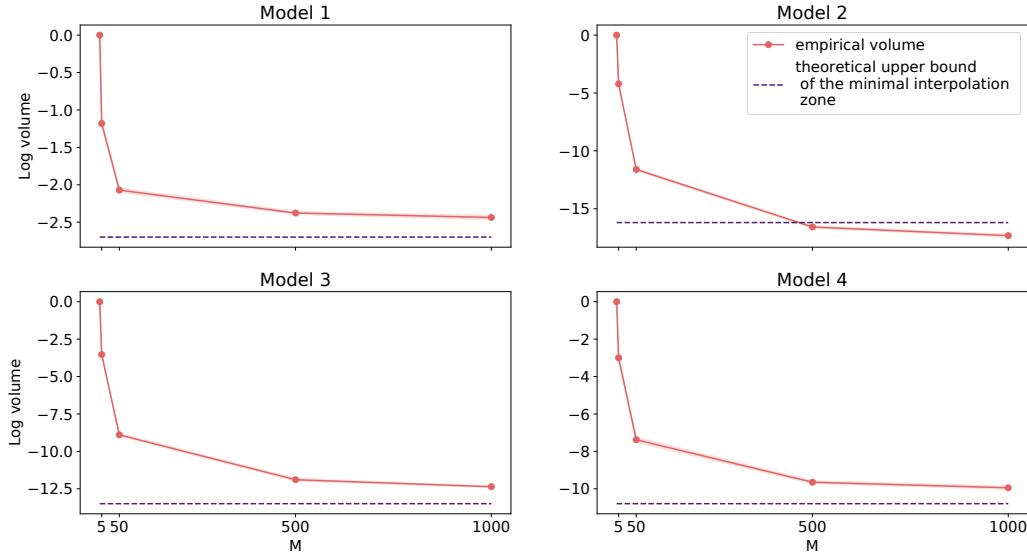


Figure 10: Log volume of Breiman RF interpolation zone w.r.t. the number M of trees. RF parameters: no bootstrap, max features = 1. Mean over 10 tries (bold line) and std (filled zone). Sample size $n = 500$.

difference between the true train labels (the Y_{i_s}) and the predicted ones (the \hat{Y}_{i_s}) by computing

$$I_{\text{loss}} := \frac{1}{n} \sum_{i=1}^n \frac{|Y_i - \hat{Y}_i|}{Y_i}.$$

The closer is this quantity to 0, the closer is the forest from interpolating. On Figure 11, we plot different quantiles of the above quantity as n varies.

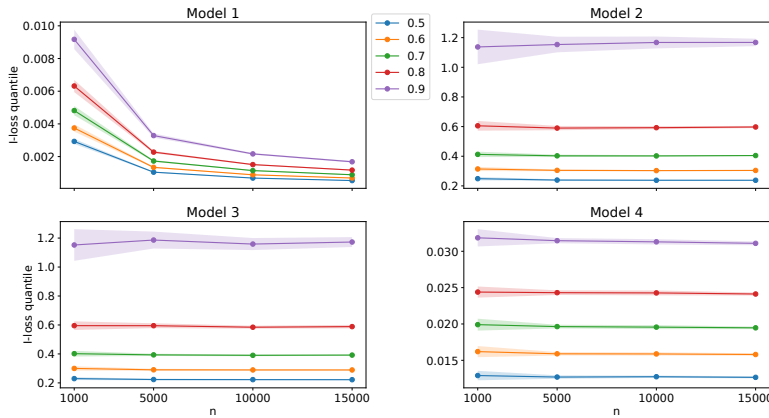


Figure 11: I_{loss} of a Breiman RF w.r.t sample size n . RF parameters: 500 trees, bootstrap on, max-features= d , max-depth set to None. Mean over 30 tries (dotted lines) and std (filled zones).

For instance, if we take the 0.8-quantile in red on Figure 11 and look at the upper-right plot (model 2), we read that the I_{loss} roughly equals 0.6 for 80% of the points. This quantity seems globally constant in n . Finally, the quantiles are smaller in the case of a strong signal-to-noise ratio (models 1 and 4) than in the case of a bigger one (models 2 and 3).

On Figure 12, we also plot the quantiles of the I_{loss} for the four different models while the number of trees varies. Adding trees does not significantly change the value of the different quantiles.

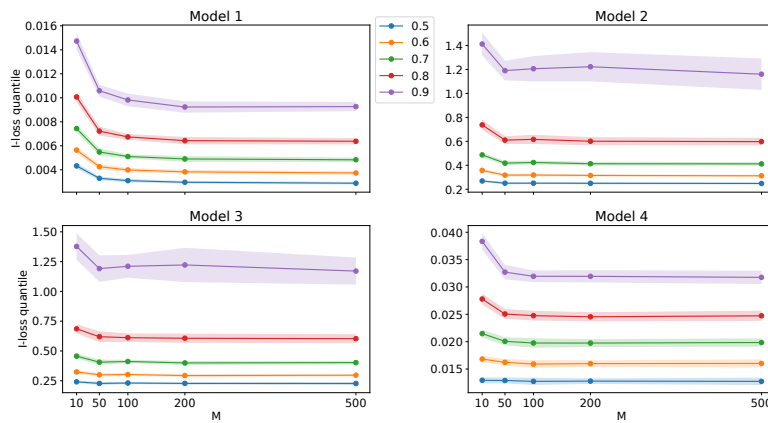


Figure 12: I_{loss} of a Breiman RF w.r.t number of trees. Parameters: bootstrap on, max-features= d , max-depth set to None. Sample size $n = 1000$. Mean over 30 tries (dotted lines) and std (filled zones).